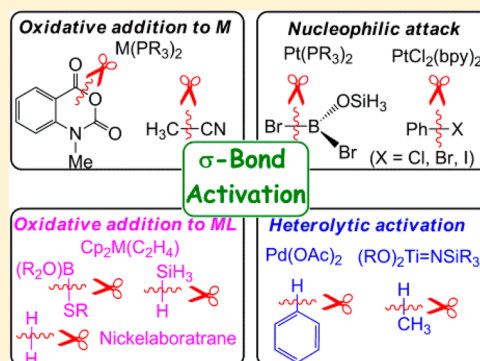


# $\sigma$ -Bond Activation of Small Molecules and Reactions Catalyzed by Transition-Metal Complexes: Theoretical Understanding of Electronic Processes

Wei Guan, Fareed Bhasha Sayyed, Guixiang Zeng, and Shigeyoshi Sakaki\*

Fukui Institute for Fundamental Chemistry, Kyoto University, Takano-Nishi-hiraki-cho 34-4, Sakyo-ku, Kyoto 606-8103, Japan

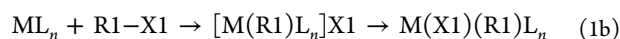
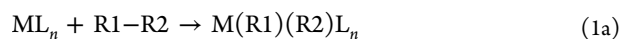
**ABSTRACT:**  $\sigma$ -Bond activations of R1–R2 and R1–X1 (R1, R2 = H, alkyl, aromatics, etc.; X1 = electronegative group) by transition-metal complexes are classified into two main categories:  $\sigma$ -bond activation by a metal (M) center and that by a metal–ligand bond. The former is classified into two subcategories: concerted oxidative addition to M and stepwise oxidative addition via nucleophilic attack of M. The latter is also classified into two subcategories: heterolytic activation by M–X2 (X2 = anion ligand) and oxidative addition to M–L (L = neutral ligand). In the concerted oxidative addition, charge transfer (CT) occurs from the M d orbital to the  $\sigma^*$  antibonding orbital of R1–R2, the clear evidence of which is presented here. The concerted oxidative additions of Ph–CN, Me–CN, and Ph–Cl to a nickel(0) complex are discussed as examples. The stepwise oxidative addition occurs through nucleophilic attack of M to R1–X1 to form an ion-pair intermediate. In the nucleophilic attack, CT occurs from the M  $d_{\sigma}$  to either the  $\sigma^*$  orbital or empty  $p_{\pi}$  orbital of R1–X1. Solvation plays a crucial role in stabilizing the transition state and ion-pair intermediate. The oxidative addition reactions of Ph–I, CH<sub>3</sub>–Br, and Br<sub>2</sub>B(OSiH<sub>3</sub>) to platinum(0), platinum(II), and palladium(0) complexes are discussed. In the heterolytic activation of R1–R2 by an M–X2 bond, R1 and R2 are bound with M and X2, respectively, indicating that R1 becomes anion-like and R2 becomes cation-like. CT mainly occurs from the X2 ligand to the  $\sigma^*$  antibonding orbital of R1–R2 and also from R1 to the M empty d orbital. In the oxidative addition to an M–L moiety, R1 is bound with M, R2 is bound with L, and thus-formed L–R2 is bound with M. The oxidative addition reaction of the Si–H bond of silane to Cp<sub>2</sub>Zr(C<sub>2</sub>H<sub>4</sub>) and that of the H–H bond of H<sub>2</sub> to Ni[MesB(*o*-Ph<sub>2</sub>PC<sub>6</sub>H<sub>4</sub>)<sub>2</sub>] are discussed as examples. The importance of the  $\sigma$ -bond activation in such catalytic reactions as nickel(0)-catalyzed phenylcyanation of alkyne, nickel(0)-catalyzed carboxylation of phenyl chloride, ruthenium(II)-catalyzed hydrogenation of carbon dioxide, and the Hiyama cross-coupling reaction is discussed based on theoretical studies.



## 1. INTRODUCTION

$\sigma$ -Bond activation reactions of small molecules by transition-metal complexes attract a lot of interest in inorganic, organometallic, and catalytic chemistries.<sup>1</sup> In our understanding,  $\sigma$ -bond activation reactions are classified into two main categories; one is  $\sigma$ -bond activation through oxidative addition to a metal, and the other is  $\sigma$ -bond activation through metathesis in which both the metal (M) and ligand (L) participate.<sup>2</sup>

The former is further classified into two subcategories:<sup>2</sup> one is concerted oxidative addition to metal (eq 1a).



where R1 and R2 represent H, alkyl, aromatics, etc., and X1 is an electronegative group such as halogen. In this reaction, the  $\sigma$  bond of R1–R2 reacts with M and bond breaking occurs in a concerted manner to afford a cis product containing M–R1 and M–R2 bonds, in general. Because R1 and R2 bound with a metal atom are considered to be anions in a formal sense, one can understand that the neutral R1 and R2 turn into anion-like

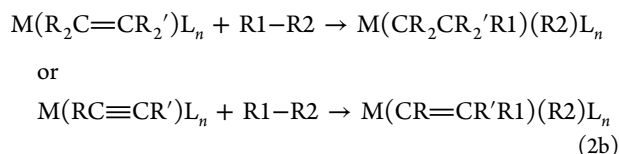
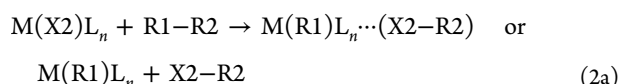
species in the reaction. In this sense, the metal oxidation state increases by 2+ and the  $\sigma$  bond of R1–R2 is broken in a homolytic manner; note that the term “homolytic scission” does not mean radical scission. This is named “concerted oxidative addition to M” hereafter. Another is a stepwise reaction, which is possible when an electronegative X1 group is bound with R1; see eq 1b. The first step is nucleophilic attack of M to R1–X1 to form an ion-pair intermediate,  $[M(R1)L_n]^+(X1)^-$ , and the second step is the binding of X1 with M. A trans product can be directly formed in this reaction. The metal oxidation state increases by 2+ in a formal sense. This is named here “stepwise oxidative addition via nucleophilic attack of M”.

The metathesis is classified into two subcategories, depending on the nature of the ligand:<sup>2</sup>

**Special Issue:** Insights into Spectroscopy and Reactivity from Electronic Structure Theory

**Received:** February 12, 2014

**Published:** April 30, 2014



When a metal and an anionic  $X_2$  ligand react with the  $\sigma$  bond of  $R_1-R_2$ , either  $M(R_1)L_n \cdots (X_2-R_2)$  or  $M(R_1)L_n + X_2-R_2$  is formed as a product, as shown in eq 2a; note that  $X_2-R_2$  interacts with  $M$  or dissociates from  $M$ , depending on the character of  $X_2-R_2$ . In the product,  $R_1$  and  $R_2$  are considered to be anion-like and cation-like, respectively, because they are bound with  $M$  and the anionic  $X_2$  ligand. This means that the  $\sigma$  bond of  $R_1-R_2$  is broken in a heterolytic manner, where the metal oxidation state does not change at all. This is called “heterolytic  $\sigma$ -bond activation” here, which is also named internal electrophilic substitution (IES), concerted metalation–deprotonation (CMD), or ambiphilic metal–ligand activation (AMLA). The name has not been fixed yet, to our knowledge.

When a neutral ligand such as alkene participates in the  $\sigma$ -bond activation,  $R_2$  and  $CR_2CR'_2R_1$  are bound with  $M$  in a product. In the case of alkyne,  $R_2$  and  $CR=CR'R_1$  are bound with  $M$  in a product; see eq 2b. Because both of them are considered anionic, the metal oxidation state increases by 2+ in a formal sense, indicating that this is understood to be concerted oxidative addition to an  $M-L$  moiety. This type of oxidative addition was first recognized in theoretical studies.<sup>3,4</sup> Although the experimental examples of this oxidative addition have been limited, the electronic process of this reaction is interesting. This is named “concerted oxidative addition to  $M-L$ ” here.

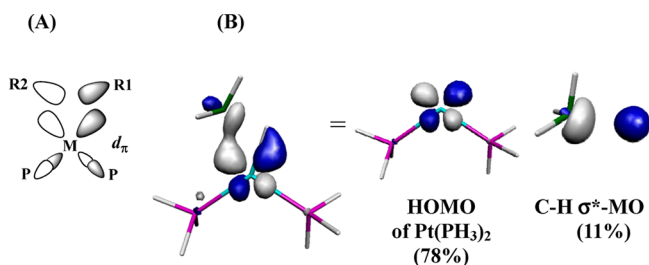
In this Forum Article, we discuss electronic processes and characteristic features of these  $\sigma$ -bond activation reactions and several catalytic reactions including them.

## 2. CONCERTED OXIDATIVE ADDITION TO METAL

### 2.1. Orbital Interaction and Geometry of the Transition State (TS).

A theoretical study of concerted oxidative addition was very previously started, and orbital interaction was discussed.<sup>5</sup> Here, we discuss briefly the important orbital interaction. As shown in Scheme 1A, charge transfer (CT) from the metal  $d_\pi$  orbital to the antibonding  $\sigma^*$  orbital of  $R_1-R_2$  is important in concerted oxidative addition.<sup>5</sup> The calculated electron population changes are consistent with this CT interaction. Also, clear theoretical evidence has been presented in our recent theoretical work of the oxidative

**Scheme 1.** CT Interaction in Concerted Oxidative Addition of the C–H Bond to  $Pt(PH_3)_2$ <sup>6</sup>



addition of  $H-CH_3$  to  $Pt(PH_3)_2$ .<sup>6</sup> Fragment molecular orbital analysis clearly indicates that the highest occupied molecular orbital (HOMO) of the TS mainly consists of the occupied  $d_\pi$  orbital of platinum and the unoccupied  $\sigma^*$ -antibonding orbital of the C–H bond of  $H-CH_3$ , as shown in Scheme 1B. This HOMO feature shows that CT occurs from the Pt  $d_\pi$  orbital to the  $\sigma^*$ -antibonding orbital of the C–H bond in the TS.

This CT interaction leads to our expectation that the TS is planar in oxidative addition to  $ML_2$  ( $M = Pt^0$  or  $Pd^0$ ;  $L =$  phosphine), as follows: The  $L-M-L$  angle is about  $140-160^\circ$  in the TS of the concerted oxidative addition. In such geometry, the HOMO of  $ML_2$  is a  $d_\pi$  orbital because it is destabilized in energy by the lone-pair orbital of  $L$ ; see Scheme 1A. Thus, it overlaps well with the  $\sigma^*$ -antibonding orbital of  $R_1-R_2$  when  $R_1-R_2$  is coplanar with the  $L-M-L$  plane. This means that CT is stronger in a planar TS than in a nonplanar TS. Actually, a planar TS has been reported in the oxidative additions of  $H-H$  and  $C-H$  bonds to  $Pt(PH_3)_2$ ,<sup>7</sup>  $Ni(PH_3)_2$ ,<sup>8</sup> and  $Pd(PH_3)_2$ .<sup>9</sup> However, a nonplanar TS was unexpectedly found in the oxidative additions of  $CH_3-CH_3$  and  $CH_3-SiH_3$  to  $Pt(PH_3)_2$ .<sup>10</sup> To uncover the origin of the nonplanar TS, a systematic study on the concerted oxidative addition of  $R-CH_3$  [ $R = CH_3, SiH_3, SiCl_3,$  or  $Si(CH_3)_3$ ] to  $Pt(PH_3)_2$  was carried out.<sup>10</sup> The activation energy ( $E_a$ ) and the dihedral angle ( $\delta$ ) between the  $P-Pt-P$  plane and the  $C-R$  bond are listed in Table 1. CT from the  $d$  orbital of platinum to the  $\sigma^*$ -

**Table 1.**  $E_a$  (in kcal/mol) for the Oxidative Addition of  $R-H$  and  $R-CH_3$  [ $R = CH_3, SiH_3, SiCl_3,$  or  $Si(CH_3)_3$ ] to  $Pt(PH_3)_2$  and  $\delta$  (in deg)

Substrate	$\delta$	$E_a$	$E_a$ ( $\delta=0$ ) <sup>a)</sup>
$CH_3-CH_3$	80	57.4	63.2
$SiH_3-CH_3$	70	19.5	27.6
$SiCl_3-CH_3$	84	15.5	28.1
$Si(CH_3)_3-CH_3$	76	23.2	34.6

nonplanar TS  
 $\delta =$  angle between  $P-Pt-P$  and  $R-Pt-C$  planes

<sup>a)</sup>The planar TS was optimized under the assumption of  $\delta = 0$ ; in other words, it is not a pure TS exhibiting imaginary frequencies of more than 2.

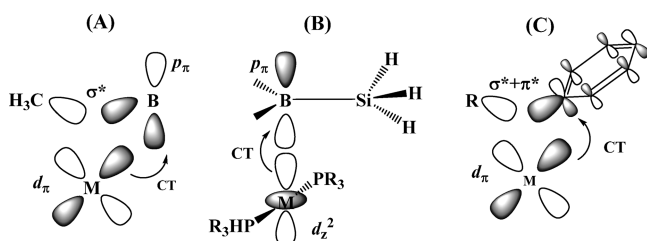
antibonding orbital of the C–R bond is larger in the planar TS than in the nonplanar TS, as expected. However, the  $E_a$  value is smaller in the nonplanar TS than in the planar TS. These results suggest that the electronic effect is not solely responsible for concerted oxidative addition. The relationship between the extent of nonplanarity and the  $E_a$  value suggests that the TS becomes nonplanar when steric repulsion between  $R_1-R_2$  and  $ML_2$  is large. Also, the IRC calculation clearly shows that a nonplanar geometry starts to change to a planar one when  $Si-C$   $\sigma$ -bond breaking starts. These results suggest that the TS becomes nonplanar when steric repulsion is large and the  $\sigma$  bond is not weakened very much in the TS. These factors are important in discussing and understanding the geometry and characteristic feature of the TS of the concerted oxidative addition reaction.

### 2.2. Concerted Oxidative Addition of a Substrate Bearing a $\pi$ -Electron System.

When a substrate has either an empty  $p$  or  $\pi^*$  orbital, this orbital participates in CT interaction from the occupied  $d$  orbital of the metal to the  $\sigma^*$ -antibonding orbital of the substrate. One good example is the oxidative addition of  $(HO)_2B-EH_3$  ( $E = C, Si, Ge,$  and  $Sn$ ) to

Pt(PH<sub>3</sub>)<sub>2</sub>.<sup>11</sup> Its TS is nearly planar when E = C but nonplanar when E = Si, Ge, or Sn. In the case of E = C, CT occurs from Pt(PH<sub>3</sub>)<sub>2</sub> to the  $\sigma^*$ -antibonding orbital of the B–C bond as well as to the empty  $p_\pi$  orbital of the B atom, as shown in Scheme 2A. In the other substrates, CT occurs to the  $p_\pi$  orbital

**Scheme 2.** CT Interaction from  $d_\pi$  or  $d_\sigma$  of the Metal to the  $\sigma^*$  or  $p_\pi$  Orbital of the Substrate



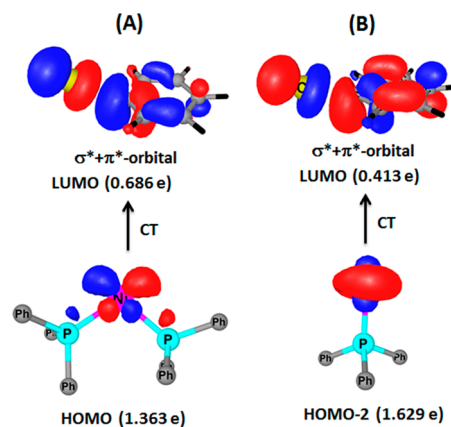
of the B atom, as shown in Scheme 2B. This nonplanar TS of E = Si, Ge, and Sn is understood to arise from two factors discussed above: The steric repulsion between Pt(PH<sub>3</sub>)<sub>2</sub> and the substrate is larger in these substrates than in E = C because CH<sub>3</sub> is smaller than SiH<sub>3</sub>, GeH<sub>3</sub>, and SnH<sub>3</sub>. Also, the TS of the B–C oxidative addition is product-like, but those of the other substrates are reactant-like because the B–C bond is stronger than the B–Si, B–Ge, and B–Sn bonds and the Pt–CH<sub>3</sub> bond is weaker than the Pt–SiH<sub>3</sub>, Pt–GeH<sub>3</sub>, and Pt–SnH<sub>3</sub> bonds. Consistent with these features, the oxidative additions of the B–Si, B–Ge, and B–Sn bonds occur with either a very small activation barrier or no barrier. Another important result is that the oxidative addition of the B–C bond occurs with a smaller activation energy than that of the C–C bond, although the B–C bond is stronger than the C–C bond. This smaller activation energy arises from two factors; one is that the  $\sigma^*$  orbital of the B–C bond exists at a lower energy than the  $\sigma^*$  orbital of the C–C bond. Another is the presence of the empty  $p_\pi$  orbital on the B atom; note that this  $p_\pi$  orbital participates in CT from the metal d orbital to the substrate, as shown in Scheme 2A.

The oxidative addition of aryl halides is important because aryl halides are often used as important substrates in many catalytic reactions such as cross-coupling reaction. Ariafard and Li<sup>12</sup> investigated the oxidative additions of CH<sub>3</sub>–Br, Ph–Br, PhCH<sub>2</sub>–Br, and CH<sub>2</sub>=CHBr to Pd(PH<sub>3</sub>)<sub>2</sub> and observed that the activation energy decreases in the order CH<sub>3</sub>–Br >

PhCH<sub>2</sub>Br > Ph–Br > CH<sub>2</sub>=CHBr. According to their explanation, the activation energy is smaller in the oxidative addition of the C(sp<sup>2</sup>)–Br bond than in that of the C(sp<sup>3</sup>)–Br bond because the  $\sigma^* + \pi^*$  orbital of the C(sp<sup>2</sup>)–Br bond overlaps better with the metal d orbitals than does the  $\sigma^*$  orbital of the C(sp<sup>3</sup>)–Br bond.

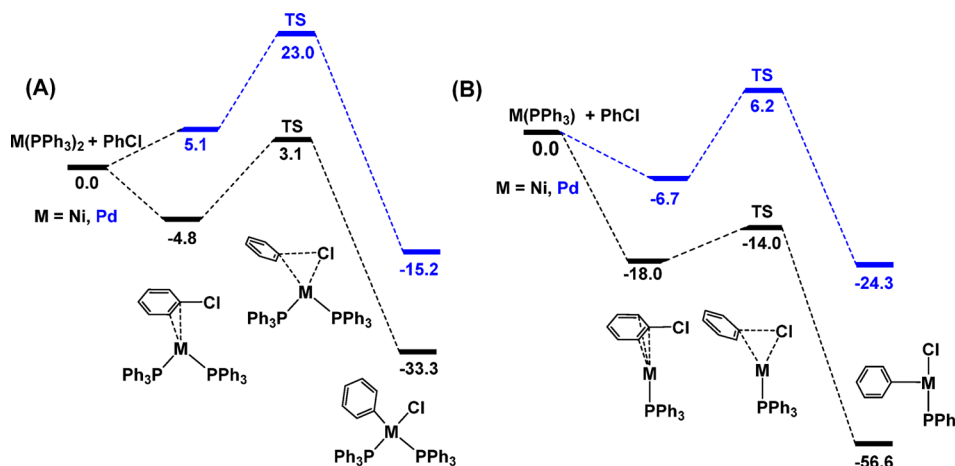
A detailed analysis was made in the oxidative addition of phenyl chloride (PhCl) to M(PH<sub>3</sub>)<sub>2</sub> (M = Ni or Pd).<sup>13</sup> Prior to oxidative addition, one of the C–C bonds of the phenyl ring coordinates with M(PH<sub>3</sub>)<sub>2</sub> in an  $\eta^2$ -coordination mode to afford a precursor complex M( $\eta^2$ -PhCl)(PH<sub>3</sub>)<sub>2</sub>, as shown in Scheme 3A. Ni( $\eta^2$ -PhCl)(PH<sub>3</sub>)<sub>2</sub> is more stable than the palladium analogue. This complex is formed through the usual donation and back-donation interactions. The Gibbs activation energy ( $\Delta G^\ddagger$ ), which is the difference in energy between the TS and the  $\eta^2$ -precursor complex, is significantly smaller in Ni(PH<sub>3</sub>)<sub>2</sub> than in Pd(PH<sub>3</sub>)<sub>2</sub>. In the TS, CT occurs from the metal  $d_\pi$  orbital to the  $\sigma^* + \pi^*$  orbital of the Ph–Cl bond, which consists of the  $\sigma^*$ -antibonding orbital of the C–Cl bond and the  $\pi^*$  orbital of the phenyl group, as shown in Scheme 4A.

**Scheme 4.** CT Interactions in the TS of the Oxidative Addition of Ph–Cl to Ni(PH<sub>3</sub>)<sub>2</sub> (A) and Ni(PH<sub>3</sub>) (B)<sup>13</sup>



The Ph–Cl bond is bent from the phenyl plane by 31.4°. Because of this bending, mixing between the  $\pi^*$  and  $\sigma^*$  orbitals occurs to afford the  $\sigma^* + \pi^*$  hybrid orbital. The fragment molecular orbital analysis indicates that the amount of CT to the  $\sigma^* + \pi^*$  hybrid orbital is 0.686e and 0.527e for nickel and

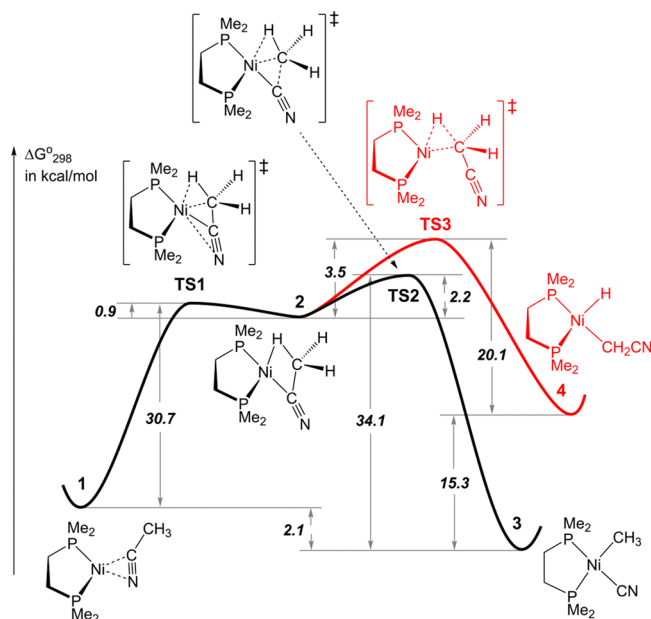
**Scheme 3.** Energy Changes in the Oxidative Addition of Ph–Cl to M(PH<sub>3</sub>)<sub>2</sub> and M(PH<sub>3</sub>) (M = Ni or Pd)<sup>13</sup>



palladium, respectively. Reverse CT of 0.171e and 0.117e moderately occurs from the  $\pi$  orbital of Ph to Ni(PPh<sub>3</sub>)<sub>2</sub> and Pd(PPh<sub>3</sub>)<sub>2</sub>, respectively. The larger CT from Ni(PPh<sub>3</sub>)<sub>2</sub> to PhCl than that from Pd(PPh<sub>3</sub>)<sub>2</sub> arises from the higher energy of the  $d_{\pi}$  orbital of Ni(PPh<sub>3</sub>)<sub>2</sub> than that of Pd(PPh<sub>3</sub>)<sub>2</sub>; in this case, the size of the d orbital is not very important because the 4d orbital of the Pd atom is larger than the 3d orbital of Ni atom but CT is smaller in Pd(PPh<sub>3</sub>)<sub>2</sub> than in Ni(PPh<sub>3</sub>)<sub>2</sub>. Because larger CT leads to smaller  $\Delta G^{\ddagger}$  values in many cases, the  $\Delta G^{\ddagger}$  value becomes smaller in the reaction of Ni(PPh<sub>3</sub>)<sub>2</sub> than in that of Pd(PPh<sub>3</sub>)<sub>2</sub>; note that the higher  $d_{\pi}$  orbital energy stabilizes the precursor complex by stronger back-donation but stabilizes the TS more than the precursor complex because CT is usually stronger in the TS than in the precursor complex because of the more distorted geometry in the TS than in the precursor complex.

Another example is oxidative addition of the C–CN  $\sigma$  bond of organic nitrile to a low-valent transition-metal complex. This is interesting because a stronger C–CN  $\sigma$  bond than the usual C(sp<sup>3</sup>)–C(sp<sup>3</sup>) bond is activated in this reaction. Also, the C–CN  $\sigma$ -bond activation is important because this reaction can be utilized for organic syntheses of acrylonitrile derivatives, as will be discussed below. Jones and his co-workers experimentally and theoretically investigated C–CN and C–H  $\sigma$ -bond activations of acetonitrile by a nickel(0) complex.<sup>14</sup> They experimentally found that [Ni(dippe)H]<sub>2</sub> [dippe = bis-(diisopropylphosphino)ethane] undergoes only oxidative addition of the C–CN bond. Solvation effects are crucial because the C–CN bond activation was calculated to be endothermic in the gas phase but exothermic when the solvation effects were considered. This is consistent with the experimental result that C–CN activation was experimentally observed in tetrahydrofuran (THF). It is likely that the polar solvent is favorable for formation of the highly polarized Ni–CN bond. As shown in Scheme 5, C–H activation needs a larger activation energy than

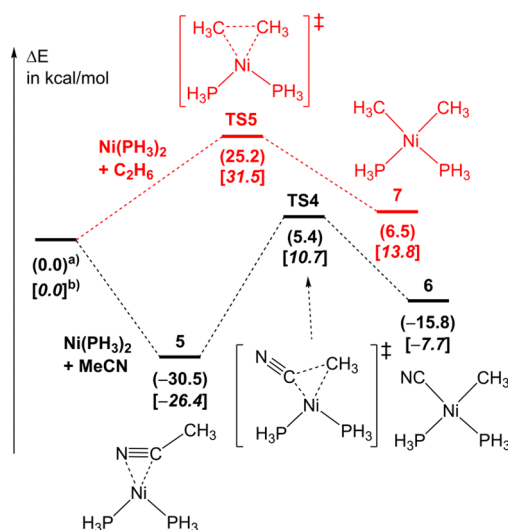
**Scheme 5.** DFT(B3LYP)-Calculated Free Energies (kcal/mol) and TSs at 298 K and 1 atm for C–C and C–H Bond Activations of Acetonitrile by Ni(dmpe) Relative to the Total Energies of Ni(dmpe) and CH<sub>3</sub>CN<sup>14</sup>



C–CN activation. Also, Ni(H)(CH<sub>2</sub>CN)(dmpe) [4; dmpe = bis(dimethylphosphino)ethane] is less stable than Ni( $\eta^2$ -MeCN)(dmpe) (1), while Ni(CN)(CH<sub>3</sub>)(dmpe) (3) is more stable than 1. These results clearly indicate that C–CN activation is kinetically and thermodynamically more favorable than C–H activation. However, the reason why C–CN activation occurs more easily than C–H activation has not been made clear.

Sakaki and his co-workers made a comparison between ethane and MeCN in the oxidative addition to Ni(PH<sub>3</sub>)<sub>2</sub> to clarify the characteristic features of the oxidative addition of the C–CN bond.<sup>15</sup> The oxidative addition of MeCN occurs with a smaller activation barrier than that of ethane, and its product, Ni(CN)(CH<sub>3</sub>)(PH<sub>3</sub>)<sub>2</sub> (6), is more stable than Ni(CH<sub>3</sub>)<sub>2</sub>(PH<sub>3</sub>)<sub>2</sub> (7) despite the stronger C–CN bond than the C–C bond, as shown in Scheme 6. It is noted that the C–

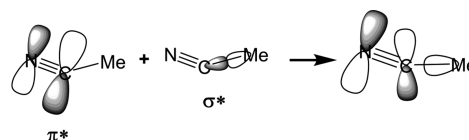
**Scheme 6.** Energy Changes (kcal/mol) in the Oxidative Addition of MeCN and C<sub>2</sub>H<sub>6</sub> to Ni(PH<sub>3</sub>)<sub>2</sub><sup>a, 15</sup>



<sup>a</sup>(a) In parentheses are the CCSD(T)-calculated energy changes. (b) In brackets are the DFT(B3PW91)-calculated energy changes.

CN bond is not coplanar to the P–Ni–P plane in TS4 in which the dihedral angle between the P–Ni–P and C–Ni–C planes is 143°, similar to that in the oxidative addition of ethane. In these oxidative addition reactions, CT occurs from the doubly occupied  $d_{\pi}$  orbital of nickel to the empty  $\sigma^*$ -antibonding orbital of MeCN and C<sub>2</sub>H<sub>6</sub>. They found that the C–CN  $\sigma$ -bond activation occurs with smaller activation energy than the C–C  $\sigma$ -bond activation because the C–CN  $\sigma^*$  orbital of the distorted MeCN exists at lower energy than the C–C  $\sigma^*$  orbital of the distorted C<sub>2</sub>H<sub>6</sub> in the TS. This is because the CN  $\pi^*$  orbital mixes into the C–CN  $\sigma^*$  orbital to lower its orbital energy than the C–C  $\sigma^*$  orbital; see Scheme 7. On the basis of these results, it should be concluded that the presence of the  $\pi^*$

**Scheme 7.** Schematic Representation of Important CT in the Oxidative Addition of MeCN to Ni(PH<sub>3</sub>)<sub>2</sub>



orbital in acetonitrile and phenyl chloride is responsible for the smaller activation energies of oxidative additions of the Ph–Cl and C–CN bonds.

**2.3. Miscellaneous Issues.** In the concerted oxidative addition, we found an important question, which of  $ML_2$  and  $ML$  is more reactive? Considering that CT from  $ML_2$  to the  $\sigma^*$ -antibonding orbital of the substrate plays a crucial role, one can expect that  $ML_2$  is more reactive than  $ML$  because two L ligands more destabilize the  $d_\pi$  orbital energy in  $ML_2$  than does one L ligand in  $ML$ . However, the oxidative addition of PhCl to monophosphine-ligated palladium(0) was experimentally reported.<sup>16</sup> The theoretical study certainly showed that the oxidative addition to  $Pd(PR_3)$  occurs more easily than that to  $Pd(PR_3)_2$ .<sup>17</sup> However, a comparison of CT interaction has not been made yet between  $ML_2$  and  $ML$ .

We investigated the oxidative addition of PhCl to the monophosphine-ligated complex  $M(PPh_3)$  ( $M = Ni$  or  $Pd$ ) and made a comparison with that to the diphosphine-ligated complex  $M(PPh_3)_2$ .<sup>13</sup> As shown in Scheme 3B, the  $\Delta G^{\ddagger}$  values of the reactions of  $Ni(PPh_3)$  and  $Pd(PPh_3)$  are smaller than those of  $Ni(PPh_3)_2$  and  $Pd(PPh_3)_2$ , respectively. This result is consistent with recent experimental and computational observations.<sup>17b</sup> It is of considerable interest to elucidate the reason why  $\Delta G^{\ddagger}$  is smaller for  $M(PPh_3)$  than for  $M(PPh_3)_2$ . Fragment molecular orbital analysis shows that CT to PhCl from  $Ni(PPh_3)$  is smaller than that from  $Ni(PPh_3)_2$ , as expected above; see Scheme 4A,B. Thus, the electronic factor is not responsible for the smaller  $\Delta G^{\ddagger}$  value in  $M(PPh_3)$  than in  $M(PPh_3)_2$ . One plausible factor is a substantially small steric repulsion between  $M(PPh_3)$  and PhCl. Another is distortion energy; in the TS of the oxidative addition to  $M(PPh_3)_2$ , the P–M–P angle must considerably decrease compared to that of the reactant to raise the metal  $d_\pi$  orbital in energy, which gives rise to a significantly large destabilization energy, as shown in Table 2. In the TS of the oxidative addition to  $M(PPh_3)$ , on the other hand, the distortion energy is negligibly small.

**Table 2. Distortion Energies (in kcal/mol) of PhCl,  $M(PPh_3)_2$ , and  $M(PPh_3)$  ( $M = Ni$  or  $Pd$ ) in the TSs of Concerted Oxidative Additions of PhCl to  $M(PPh_3)_2$  and  $M(PPh_3)$** <sup>13</sup>

	reaction with $M(PPh_3)_2$		reaction with $M(PPh_3)$	
	PhCl	$M(PPh_3)_2$	PhCl	$M(PPh_3)$
$M = Ni$	38.3	16.4	9.7	2.7
$M = Pd$	25.9	10.7	15.0	0.8

The last issue to be discussed here is the regioselectivity of the oxidative addition. Recently, nickel-catalyzed decarboxylative coupling reactions have attracted a lot of interest because various nitrogen-containing heterocycles can be synthesized by this reaction;<sup>18,19</sup> see Scheme 8A for one example. Recently, we investigated the oxidative addition of isatoic anhydride to  $Ni(PPh_3)(AL)$  ( $AL = \text{alkyne}$ ).<sup>20</sup> In this reaction, five different  $\sigma$  bonds are candidates for activation. The regioselectivity of the oxidative addition is of considerable importance because the selectivity of a product significantly depends on the regioselectivity. Taking into account the position changes of the ligands ( $AL$  and  $PMe_3$ ) in each bond activation reaction, 10 kinds of TSs must be investigated, as shown in Scheme 8B. As shown in Figure 1,  $TS1a^{AL1}$  is the most stable of all TSs, but its product  $2a^{AL1}$  is not the most stable. The next stable  $TS1a_{iso}^{AL1}$  leads to the formation of the very unstable product  $2a_{iso}^{AL1}$ .

The third stable  $TS1d^{AL1}$  provides the most stable product  $2d^{AL1}$ . However, the next decarboxylation step starting from  $2d^{AL1}$  is very difficult. On the other hand, the next step starting from  $2a^{AL1}$  occurs with the smallest activation energy, indicating that the oxidative addition via  $TS1a^{AL1}$  is a key elementary step in this catalytic reaction. The stability of the TS significantly depends on CT from the nickel  $d_\pi$  orbital to the  $\pi^*$ -antibonding orbital (lowest unoccupied molecular orbital, LUMO) of isatoic anhydride. This CT is the largest in  $TS1a^{AL1}$ . The fragment molecular orbital analysis indicates that the electron population on the LUMO of isatoic anhydride considerably increases to 0.688e in  $TS1a^{AL1}$ , and the population on the HOMO of  $Ni(PPh_3)(AL)$  considerably decreases to 1.357e. It is concluded that the regioselectivity of this concerted oxidative addition must be discussed with the LUMO feature, as expected. Also, the bond energy is an important factor in determining the stability of the product.

This type of regioselectivity has not been investigated well so far. For further development of this type of synthetic reaction, the regioselectivity of the oxidative addition must be investigated from the viewpoints of kinetic and thermodynamic factors in more detail.

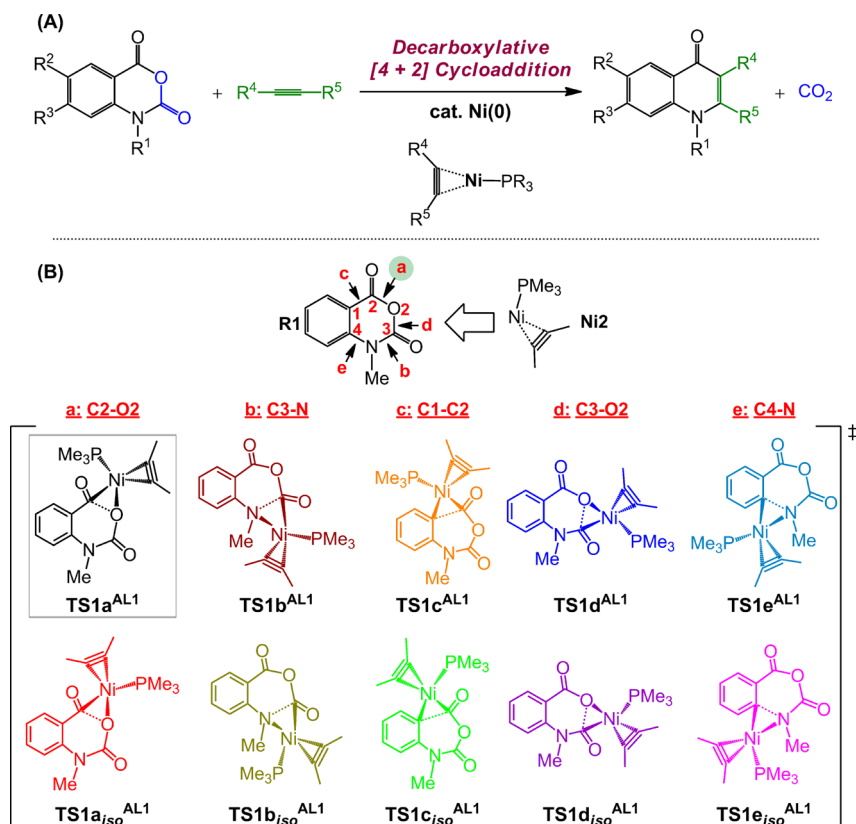
### 3. STEPWISE OXIDATIVE ADDITION VIA THE NUCLEOPHILIC ATTACK OF A METAL

In the stepwise oxidative addition, first the nucleophilic attack of a metal to a substrate occurs to form an ion-pair intermediate and then the anion is bound with the metal to form a final product.<sup>21</sup> In 2004, Senn and Zielger investigated the oxidative addition of phenyl halides to palladium(0) complexes  $Pd(P^*P)$  [ $P^*P = \text{dmpe}$  or bis(dimethylphosphino)biphenyl (bimpe); Scheme 9] and found that this reaction occurs via the concerted oxidative addition pathway in the gas phase but in a stepwise manner in a THF solution,<sup>22</sup> where the COSMO model was employed to incorporate solvation effects. They succeeded in optimizing the TS for halide dissociation from the Pd group.

The oxidative addition of  $CH_3I$  to  $Pt(bdpp)(CH_3)_2$  [ $bdpp = (2S,4S)\text{-}2,4\text{-bis}(\text{diphenylphosphino})\text{pentane}$ ] was theoretically investigated by the Kégl group,<sup>23a</sup> where the polarizable continuum model (PCM) was employed to incorporate solvation effects. They found that the reaction occurs via a TS with a collinear  $I\text{-}CH_3\text{-}Pt$  structure, which is essentially the same as that of the  $S_N2$  substitution reaction.

To explore how much the solvation effects are important, Sakaki and his co-workers investigated the oxidative addition of methyl iodide to  $cis\text{-}Pt(\text{Me})_2(\text{NH}_3)_2$ , where the solvation effects were evaluated with the reference interaction site model self-consistent-field (RISM-SCF) theory; see Scheme 10.<sup>24</sup>  $cis\text{-}Pt(\text{Me})_2(\text{NH}_3)_2$  is a model of diphenyl(2,2'-bipyridine)-platinum(II), which was employed in the pioneering work by Rendina and Puddephatt.<sup>23b</sup> Theoretical calculations show that the reaction occurs via the nucleophilic attack of the Pt center to the C atom of methyl iodide to afford an ion-pair intermediate. The TS is essentially the same as that found by the Kégl group.<sup>23a</sup> The RISM-SCF results clearly demonstrate that solvation occurs around both the Pt center and the I atom to stabilize the TS and ion-pair intermediate.

Although the importance of the solvation effect was well discussed in those works, other important factors for the stepwise oxidative addition via nucleophilic attack were unclear. Such factors have been discussed recently in the oxidative addition of the B–Br bond of  $Br_2B(\text{OSiMe}_3)$  to  $M(\text{PMe}_3)_2$  ( $M = Pt$  or  $Pd$ );<sup>25</sup> see Scheme 11. This reaction was experimentally

Scheme 8. Decarboxylative Cycloaddition of Alkyne To Form a New Nitrogen-Containing Heterocycle<sup>a,20</sup>

<sup>a</sup>Some parts of this scheme are cited from ref 20 with permission of the American Chemical Society.

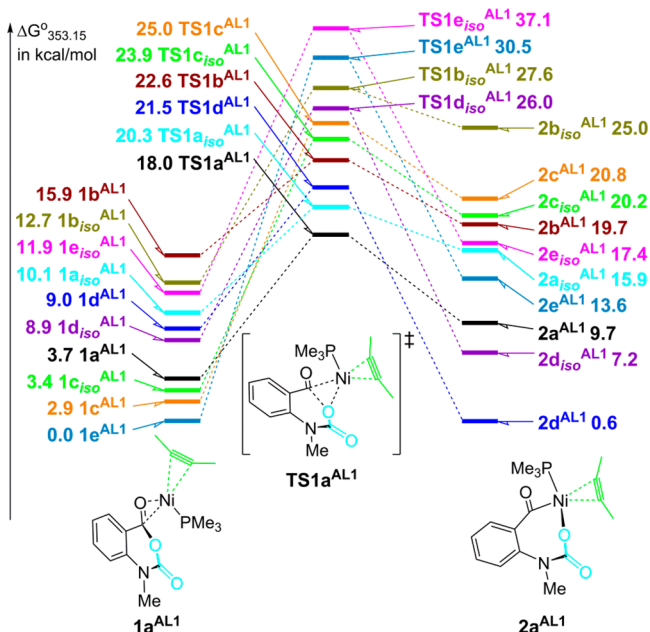
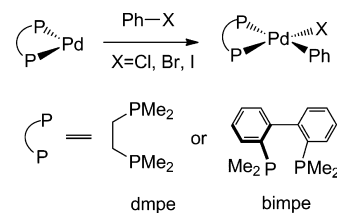
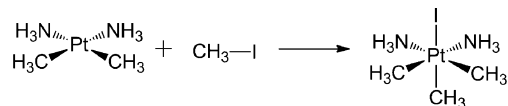


Figure 1. Energy profiles ( $\Delta G^{\circ}_{353.15}$ ) for the oxidative addition of isatoic anhydride to Ni(PMe<sub>3</sub>)(but-2-yne).<sup>20</sup>

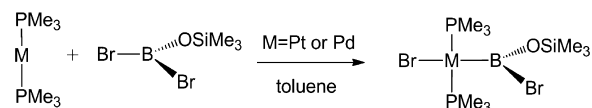
reported by Brauschweig and co-workers.<sup>26</sup> One important experimental result is that a trans product is directly produced; remember that a cis product is generally produced by the concerted oxidative addition. In the case of the platinum system, two reaction pathways were found, as shown in Figure 2. One is a stepwise oxidative addition pathway via the

Scheme 9. Oxidative Addition of Phenyl Halides to Palladium(0) Complexes Investigated by Senn and Ziegler<sup>22</sup>

## Scheme 10. Model Reaction of the Oxidative Addition of Methyl Iodide to a Platinum(II) Complex



## Scheme 11. Oxidative Addition of Bromoborane to Platinum(0) and Palladium(0) Complexes



nucleophilic attack of Pt, which directly leads to the formation of a trans product. The other is a concerted oxidative addition of the B–Br  $\sigma$  bond to Pt(PMe<sub>3</sub>)<sub>2</sub> followed by thermal cis–trans isomerization, in which the cis–trans isomerization is a rate-determining step. The former reaction pathway occurs with a lower activation barrier than the latter one. In the

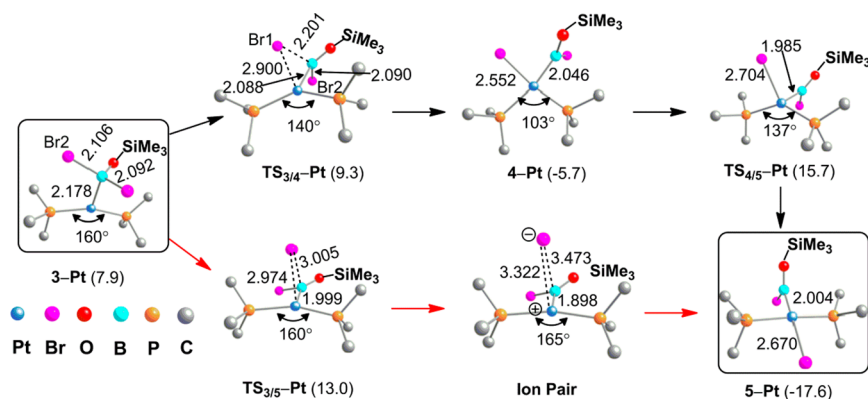


**Figure 2.** Geometry changes by the concerted oxidative addition and stepwise oxidative addition to the Pt center only in the reaction between  $\text{Br}_2\text{B}(\text{OSiMe}_3)$  and  $\text{Pt}(\text{PMe}_3)_2$ .<sup>25</sup> Some parts of this figure are taken from ref 25 with permission of the American Chemical Society.

palladium system, only the concerted oxidative addition was found with a moderate activation energy. An interesting difference is found between the TSs of the concerted oxidative addition and the stepwise one; see Figure 2. The P–Pt–P angle of  $\text{TS}_{3/5}\text{-Pt}$  (stepwise oxidative addition) is much larger than those of  $\text{TS}_{3/4}\text{-Pt}$  and  $\text{TS}_{3/4}\text{-Pd}$  (concerted oxidative addition). In the concerted oxidative addition, CT must be formed between the metal  $d_\pi$  orbital and the  $\sigma^*$ -antibonding orbital of the substrate, as was discussed in section 2.1. To form the strong CT interaction, the metal  $d_\pi$  orbital energy must become higher. To raise the  $d_\pi$  orbital energy, the P–M–P angle must become smaller in the TS; remember that the  $d_\pi$  orbital energy becomes higher by the P–M–P bending because the P–M–P bending increases the antibonding overlap of the  $d_\pi$  orbital with the lone-pair orbital of  $\text{PMe}_3$ ; see  $\text{TS}_{3/4}\text{-Pt}$  in Figure 3A. In the stepwise oxidative addition via nucleophilic

type CT.<sup>27</sup> In other words, the frontier orbital is an occupied  $d_\sigma$  orbital in the stepwise oxidative addition via nucleophilic attack and an occupied  $d_\pi$  in the concerted oxidative addition. In the platinum(0) complex, the d orbital is at a higher energy than that in the palladium(0) complex, as is well-known. Thus,  $\text{Pt}(\text{PMe}_3)_2$  does not need to induce the P–Pt–P bending to raise the d orbital energy. In  $\text{Pt}(\text{PMe}_3)_2$  bearing a large P–Pt–P angle, the  $d_\sigma$  orbital is HOMO, which is favorable for the nucleophilic attack of the Pt atom to the B atom of bromoborane; remember that the B atom has an empty  $p_\pi$  orbital, as mentioned above. On the other hand, the  $d_\sigma$  orbital energy of  $\text{Pd}(\text{PMe}_3)_2$  is not sufficiently high for nucleophilic attack. Also, the P–Pd–P bending occurs with smaller destabilization energy than the P–Pt–P bending in the platinum analogue. Because the  $d_\pi$  orbital becomes the HOMO in  $\text{Pd}(\text{PMe}_3)_2$  bearing a small P–Pt–P angle, the concerted oxidative addition becomes more favorable than the oxidative addition via nucleophilic attack. This is the reason why the stepwise oxidative addition via nucleophilic attack occurs in the platinum reaction system but the concerted one in the palladium reaction system.

The above results indicate that the following conditions are necessary for stepwise oxidative addition via nucleophilic attack: (i) the metal has an occupied  $d_\sigma$  orbital at a high energy; (ii) the substrate has an acceptor orbital extending toward M; (iii) the leaving group is electronegative like halogen; and (iv) the polar solvent is employed. The  $\sigma$ -type CT from metal to  $\eta^1$ -carbon dioxide ( $\text{CO}_2$ ) has been reported previously in cobalt(I) and rhodium(I) complexes,<sup>28</sup> which is similar to that of the TS in the stepwise oxidative addition via nucleophilic attack. Thus, the  $\eta^1\text{-CO}_2$  complexes<sup>29</sup> and similar complexes are good candidates for the stepwise oxidative addition via nucleophilic attack.

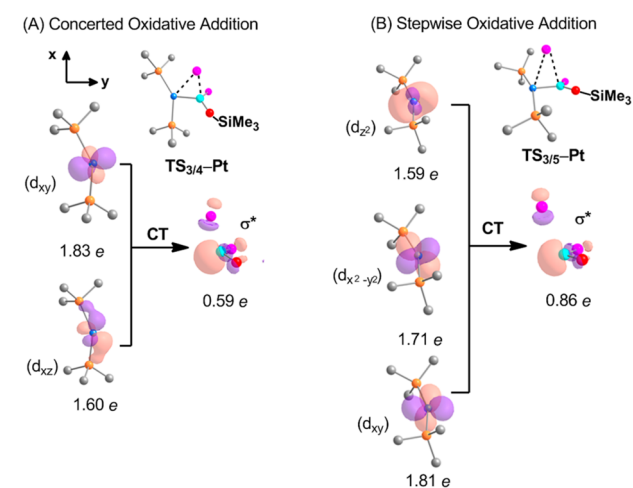


**Figure 3.** Important CT interaction in the TS of the concerted oxidative addition and stepwise oxidative addition to  $\text{Pt}(\text{PMe}_3)_2$ .<sup>25</sup> This figure is taken from ref 25 with permission of the American Chemical Society.

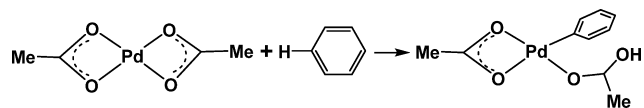
attack, the orbital interaction is different. The LUMO of  $\text{Br}_2\text{B}(\text{OSiMe}_3)$  is an empty  $p_\pi$  orbital of the B atom into which the B–Br  $\sigma^*$ -antibonding orbital mixes. Hence, CT mainly occurs from the  $d_\sigma$ -like orbital of  $\text{Pt}(\text{PMe}_3)_2$  to the LUMO; see  $\text{TS}_{3/5}\text{-Pt}$  in Figure 3B. This CT interaction in  $\text{TS}_{3/5}\text{-Pt}$  resembles well that of  $\text{Pt}(\text{PMe}_3)_2(\text{AlMe}_3)$  in which the Pt  $d_\sigma$  orbital interacts with the empty p orbital of  $\text{AlMe}_3$  to form  $\sigma$ -

#### 4. HETEROLYTIC $\sigma$ -BOND ACTIVATION BY M–X

The heterolytic  $\sigma$ -bond activation reaction is of considerable interest because a covalent R1–R2 bond is cleaved in a heterolytic manner, as mentioned in section 1. Though the heterolytic  $\sigma$ -bond activation can be found in an old experimental work,<sup>30</sup> this activation was not realized in the experimental work. Recently, this reaction has attracted a lot of interest.<sup>1a,b</sup> Here, we briefly discuss the electronic process of the heterolytic C–H  $\sigma$ -bond activation<sup>6,31</sup> to avoid overlap with the other parts of this Forum in which the C–H activation is discussed.

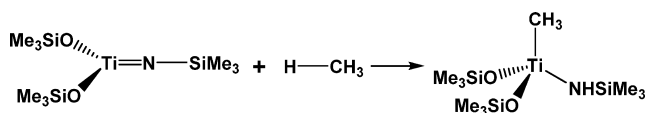
Important is the difference in the electronic process between the concerted oxidative addition and heterolytic  $\sigma$ -bond activation. A detailed analysis of the electron population changes was first made in the reactions of methane and benzene with a palladium(II) bis(formate) complex, which was a model of palladium(II) bis(acetate) employed experimentally; see Scheme 12.<sup>31</sup> The computational results show that the

**Scheme 12. Heterolytic  $\sigma$ -Bond Activation of Benzene by a Palladium(II) Acetate Complex**



hydrogen atomic population considerably decreases but the electron populations of the palladium and phenyl group considerably increase from a as the reaction occurs from a palladium(II)  $\eta^2$ -benzene precursor complex to a palladium(II) phenyl product complex. Later, more detailed analysis was made based on the orbital interaction diagram in the reaction of methane with a titanium(IV) imido complex,  $(\text{Me}_3\text{SiO})_2\text{Ti}=\text{N}(\text{SiMe}_3)$ ; see Scheme 13.<sup>6</sup> In this reaction, the hydrogen

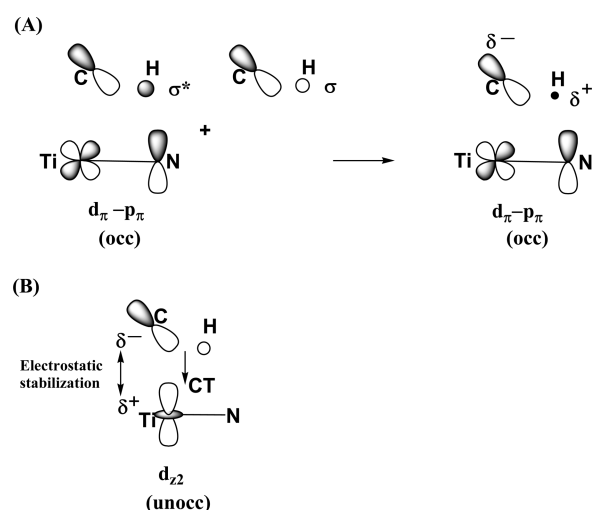
**Scheme 13. Heterolytic C–H  $\sigma$ -Bond Activation of Methane by a Titanium(IV) Imido Complex**



atomic population considerably decreases, while the electron population of  $\text{CH}_3$  considerably increases. The titanium atomic population considerably increases as the reaction occurs from a reactant to a TS and then moderately decreases as the reaction proceeds from a TS to a product. On the basis of these population changes, we believe that this reaction can be named the heterolytic  $\sigma$ -bond activation reaction. These features are in contrast with the population changes observed in the concerted oxidative addition, in which both electron populations of hydrogen and  $\text{CH}_3$  groups considerably increase and the metal atomic population considerably decreases.

The population changes are reasonably understood based on the orbital interaction shown in Scheme 14.<sup>6</sup> The HOMO of  $(\text{Me}_3\text{SiO})_2\text{Ti}=\text{N}(\text{SiMe}_3)$  is a  $d_\pi$ - $p_\pi$  bonding orbital in which the  $p_\pi$  orbital of nitrogen is a main contributor. Into this HOMO, the  $\sigma^*$ -antibonding orbital of the C–H bond of methane mixes in a bonding way because the  $\sigma^*$  orbital exists at a higher energy than the  $d_\pi$ - $p_\pi$  bonding orbital. Simultaneously, the  $\sigma$ -bonding orbital of the C–H bond mixes into this  $d_\pi$ - $p_\pi$  bonding orbital in an antibonding way because the former orbital exists at a lower energy than the latter one. These orbital mixings can be understood based on the second-order perturbation theory. Because of the overlap of the  $\sigma$ -bonding orbital with the  $\sigma^*$ -antibonding orbital, the participation of the  $1s$  orbital of hydrogen considerably decreases and the participation of the  $sp^3$  orbital of  $\text{CH}_3$  considerably increases in the HOMO of the TS. As a result, the hydrogen atomic population decreases very much but the electron population of  $\text{CH}_3$  increases very much, as discussed above. The empty  $d_z^2$  orbital of titanium interacts with the  $sp^3$  orbital of  $\text{CH}_3$  to form a CT interaction, which contributes to the

**Scheme 14. Important Orbital Interaction in the Heterolytic  $\sigma$ -Bond Activation**



increase in the titanium atomic population, the formation of the Ti– $\text{CH}_3$  bond, and the stabilization of the TS. On the basis of these computational results, it is concluded that this heterolytic  $\sigma$ -bond activation reaction occurs easily when the metal atom has an empty  $d$  orbital at a low energy and the X ligand has an occupied  $p_\pi$  orbital at a high energy.

The knowledge of these electronic processes provides the reason why this reaction is also called IES, CMD, and AMLA in theoretical and experimental works.<sup>32–34</sup> The name IES is reasonable because substitution of an electrophilic metal for the H atom of the substrate occurs in this reaction. Also, this reaction is understood in terms of metalation of the C atom concomitantly with protonation of the ligand. Hence, this can be named CMD. The final name AMLA is reasonable too because ligand participation is indispensable. Although all of these are reasonable, we believe that heterolytic activation by M–X is the best because it is more general and clearly shows the characteristic features of the electronic process. This type of heterolytic activation is found in many catalytic reactions, which will be discussed below.

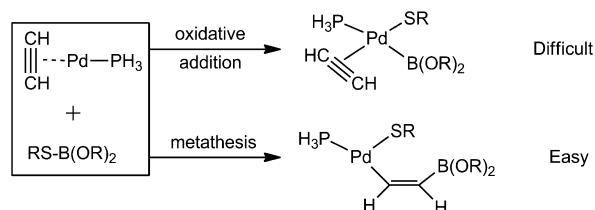
## 5. OXIDATIVE ADDITION TO M–L

Experimental and theoretical reports of the oxidative addition to M–L (L = neutral ligand such as alkyne and alkene; eq 2b) have been limited, as mentioned in section 1. However, one can expect that this reaction plays an important role in the catalytic reaction.

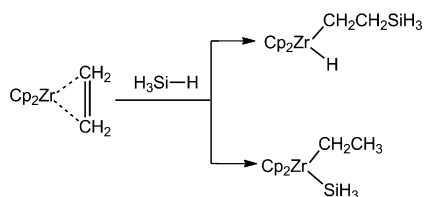
This type of oxidative addition was reported first in the theoretical work of the thio-boration of alkyne by  $\text{Pd}(\text{PH}_3)$ .<sup>3</sup> The usual concerted oxidative addition of thio-borane  $\text{RS–B}(\text{OR})_2$  does not occur in the palladium complex. In the product of the reaction between  $\text{Pd}(\text{PH}_3)(\text{C}_2\text{H}_2)$  and  $\text{RS–B}(\text{OR})_2$ , one C atom of alkyne is bound with the  $\text{B}(\text{OR})_2$  group, the other C atom is bound with the Pd atom, and also the SR group is bound with the Pd atom, as shown in Scheme 15. Although this was called metathesis,<sup>3</sup> this is understood to be the oxidative addition of  $\text{RS–B}(\text{OR})_2$  to the  $\text{Pd}-(\text{C}_2\text{H}_2)$  moiety because the Pd oxidation state increases by 2+ in a formal sense. The second example is the reaction between hydrosilane and  $\text{Cp}_2\text{Zr}(\text{C}_2\text{H}_4)$ , which is one elementary step of the hydrosilylation of alkene by  $\text{Cp}_2\text{Zr}$ ; see Scheme 16. In the product, either alkyl and silyl groups or alkyl and hydride



**Scheme 15. Oxidative Addition of the S–B Bond to the M–alkyne Moiety Found in Thioboration of Alkyne by a Palladium(0) Complex<sup>3</sup>**

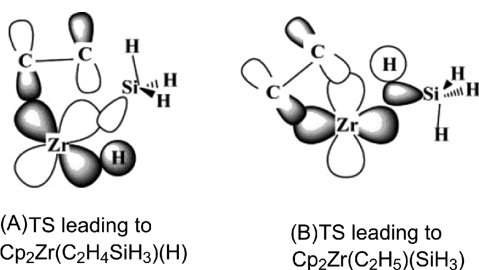


**Scheme 16. Oxidative Addition of the Si–H Bond to the M–Ethylene Moiety Found in Hydrosilylation of Ethylene by Cp<sub>2</sub>Zr<sup>4</sup>**



groups are bound with the Zr center, which indicates that the Zr oxidation state increases by 2+ in a formal sense. An important orbital interaction was discussed in that work, as shown in Scheme 17; the Si–H  $\sigma^*$ -antibonding orbital overlaps

**Scheme 17. Important Orbital Interaction in the Oxidative Addition of Silane to Cp<sub>2</sub>Zr(C<sub>2</sub>H<sub>4</sub>)<sup>a,4b</sup>**

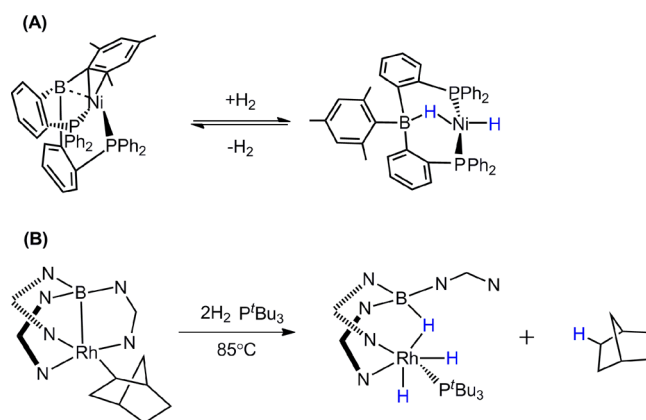


<sup>a</sup>This scheme is cited from ref 4b with permission of the American Chemical Society.

well with the  $d_{\pi}-\pi^*$  bonding orbital between Zr and C<sub>2</sub>H<sub>4</sub>, which is a usual  $\pi$ -back-donation interaction. This orbital overlap leads to the formation of Zr–alkyl and either Zr–hydride or Zr–silyl.

Recently, Peters and co-workers synthesized a nickel borane complex, Ni[MesB(*o*-Ph<sub>2</sub>PC<sub>6</sub>H<sub>4</sub>)<sub>2</sub>], and found that it facially reacts with a dihydrogen (H<sub>2</sub>) molecule to yield a *trans*-nickel(II) hydridoborohydrido complex at room temperature;<sup>35</sup> see Scheme 18A). In this complex, borane plays the role of a  $\sigma$ -acceptor ligand, which is often called a Z-type ligand.<sup>36</sup> The  $\sigma$ -bond activation of H–H by this nickel complex was theoretically investigated recently, as shown in Figure 4.<sup>37</sup> In Ni[MesB(*o*-Ph<sub>2</sub>PC<sub>6</sub>H<sub>4</sub>)<sub>2</sub>], the 3d, 4s, and 4p orbital populations of the Ni atom are similar to those of the typical nickel(II) complex, indicating that strong Ni  $\rightarrow$  B CT interaction is formed. However, the nickel 3d and 4p orbital populations considerably increase when H<sub>2</sub> coordinates with the Ni center, indicating that the Ni atom becomes electron-rich. Then, 1,2-addition of the H–H  $\sigma$  bond across the Ni–B bond occurs to form a hydridoborohydrido complex, where the electron-rich

**Scheme 18. H–H  $\sigma$ -Bond Activation by a Nickel(0) Borane Complex and a Rhodium(I) Complex<sup>35,36</sup>**



Ni center and electron-deficient borane ligand work in a cooperative manner. In the TS, CT occurs from the  $\sigma$ -bonding orbital of H<sub>2</sub> to the  $\sigma^*$ -antibonding orbital of the Ni–B bond. Also, reverse CT occurs from the nickel  $d_{x^2-y^2}$  orbital to the  $\sigma^*$ -antibonding orbital of H<sub>2</sub>. The former CT (0.683e) is much larger than the latter one (0.284e); see Scheme 19. As the reaction proceeds from the TS to the product, the positively charged H atoms receive electron population from the Ni atom to form the nickel(II) hydridoborohydrido complex. In this reaction step, the oxidation state of the Ni atom increases by 2+. These electronic processes are different from those of the concerted oxidative addition and also heterolytic  $\sigma$ -bond activation. Although the total reaction can be understood to be the oxidative addition to M–L, the electronic process is not simple in the case of a metal complex with the Z-type ligand.

We believe that the oxidative addition to M–L must be investigated more in various cases because the electronic process of this reaction is not simple, and this reaction exhibits the potential for constructing a new catalytic reaction. Actually, the metal–borane bond is reactive for other  $\sigma$ -bond activations; the Parkin group reported 1,2-addition reactions of a variety of dihalogen molecules across the Ni–B bond.<sup>38</sup> The Owen group succeeded the reaction of a rhodium(I) borane complex with two H<sub>2</sub> molecules to produce a rhodium(III) dihydridoborohydrido complex; see Scheme 18B.<sup>39</sup> The theoretical investigation of these reactions should be performed more.

## 6. CATALYTIC REACTIONS INVOLVING $\sigma$ -BOND ACTIVATION AS THE KEY ELEMENTARY STEP

As is well-known, the  $\sigma$ -bond activation reaction is involved as a crucial process in many catalytic reactions. In this section, we report several computational results of such catalytic reactions.

**6.1. Catalytic Reactions via the Concerted Oxidative Addition to a Metal. A. Nickel(0)-Catalyzed Phenylcyanation of Alkyne.** Nickel(0)-catalyzed phenylcyanation of alkyne was experimentally succeeded by Nakao, Hiyama, and their co-workers.<sup>40</sup> This catalytic reaction is of considerable interest because the strong Ph–CN bond is broken and a new acrylonitrile derivative is synthesized. The experimental and computational studies reported that the  $\sigma$ -bond activations of Me–CN and Ph–CN occur through the concerted oxidative addition mechanism. It is likely to consider that the first step is the oxidative addition of benzonitrile (PhCN) to Ni-(phosphine)<sub>2</sub> to form a nickel(II) phenylcyano complex, Ni(CN)(Ph)(phosphine)<sub>2</sub>. This reaction was theoretically

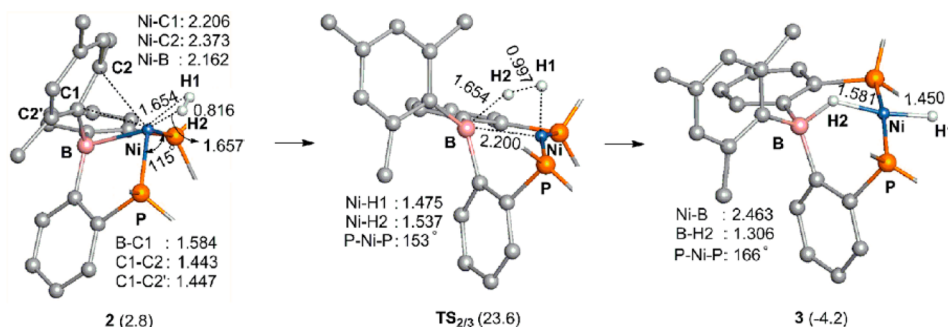
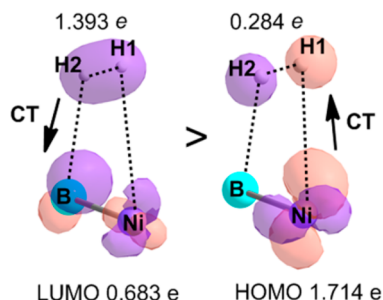


**Figure 4.** Geometry changes in the oxidative addition of a H<sub>2</sub> molecule to a nickel(0) borane complex.<sup>37</sup> Distances are in angstroms and angles in degrees. Some parts of this figure are taken from ref 37 with permission of the American Chemical Society.

**Scheme 19. CT Interactions in the TS of the H–H  $\sigma$ -Bond Activation by a Nickel(0) Borane Complex<sup>a,37</sup>**



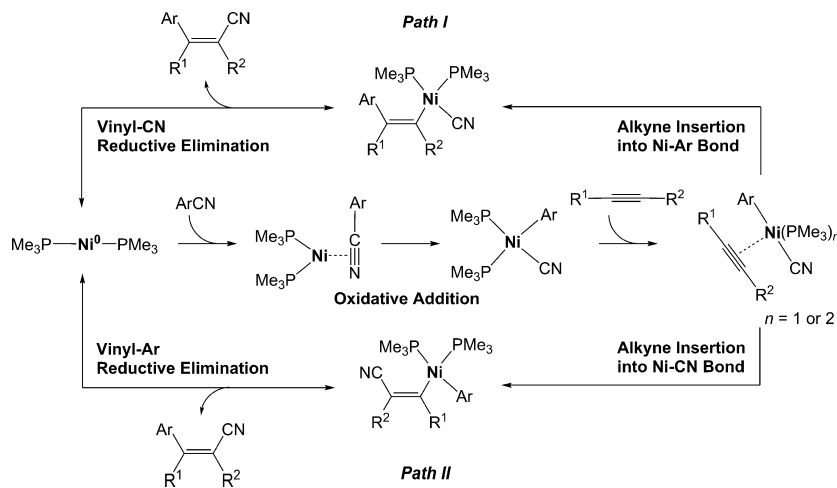
<sup>a</sup>This scheme is cited from ref 37 with permission of the American Chemical Society.

investigated with a nickel(0) chelate phosphine complex such as Ni(dmpe) by Jones and co-workers.<sup>41</sup> However, Ni(PMe<sub>3</sub>)<sub>2</sub> was used in the catalytic reaction,<sup>40</sup> indicating that something is different between Ni(PMe<sub>3</sub>)<sub>2</sub> and Ni(dmpe). Also, there are many possibilities in its catalytic cycle, for instance, which of the Ni–CN and Ni–Ph bonds undergoes alkyne insertion, which elementary step is rate-determining, how the Ph–CN bond activation occurs, and so on; see Scheme 20. Sakaki and co-workers theoretically investigated Ni(PMe<sub>3</sub>)<sub>2</sub>-catalyzed phenylcyanation of alkyne to clarify the reaction mechanism.<sup>42</sup> As shown in Figure 5, the most stable precursor complex is an  $\eta^2$ -CN-coordinated PhCN complex, Ni(PMe<sub>3</sub>)<sub>2</sub>( $\eta^2$ -NCPh) (1).

Because the C–CN  $\sigma$ -bond activation cannot directly occur from 1, 1 isomerizes to an  $\eta^2$ -aryl intermediate, 2, prior to the C–CN  $\sigma$ -bond activation (1  $\rightarrow$  TS1  $\rightarrow$  2). This isomerization requires a large  $\Delta G^{\ddagger}$  value. The similar geometry changes were reported by Jones and co-workers in their theoretical study of the oxidative addition of Ph–CN to Ni(dmpe).<sup>41</sup> However, the  $\Delta G^{\ddagger}$  value is considerably larger than that in the case of Ni(PMe<sub>3</sub>)<sub>2</sub>.<sup>41</sup> This is because Ni(PMe<sub>3</sub>)<sub>2</sub> is more flexible than Ni(dmpe) bearing a bidentate chelate ligand. Hence, Ni(PMe<sub>3</sub>)<sub>2</sub> is a better catalyst than Ni(chelate phosphine). Starting from 2, the oxidative addition occurs with a moderate activation barrier to afford Ni(CN)(Ph)(PMe<sub>3</sub>)<sub>2</sub> (3). Then, alkyne coordinates with the Ni center to form a five-coordinate intermediate, 4, followed by alkyne insertion into the Ni–Ph bond. The alkyne insertion into the Ni–CN bond is much more difficult than that into the Ni–Ph bond. Finally, reductive elimination of PhCH=CH–CN occurs from either a mono- or a diphosphine intermediate. The rate-determining step is the oxidative addition of Ph–CN to Ni(PMe<sub>3</sub>)<sub>2</sub>. These results clearly show that the nickel(0) complex can be utilized for various catalytic reactions including the concerted oxidative addition because it is reactive for a strong C–CN bond. Important is whether the next step occurs easily or not.

**B. Nickel(0)-Catalyzed Carboxylation of Phenyl Chloride with CO<sub>2</sub>.** The use of CO<sub>2</sub> to synthesize carboxylic acid is of much recent interest because of the low toxicity and low cost of CO<sub>2</sub>. However, successful reports of direct carboxylation of aryl

**Scheme 20. Possible Catalytic Cycles of Nickel(0)-Catalyzed Phenylcyanation of Alkyne**



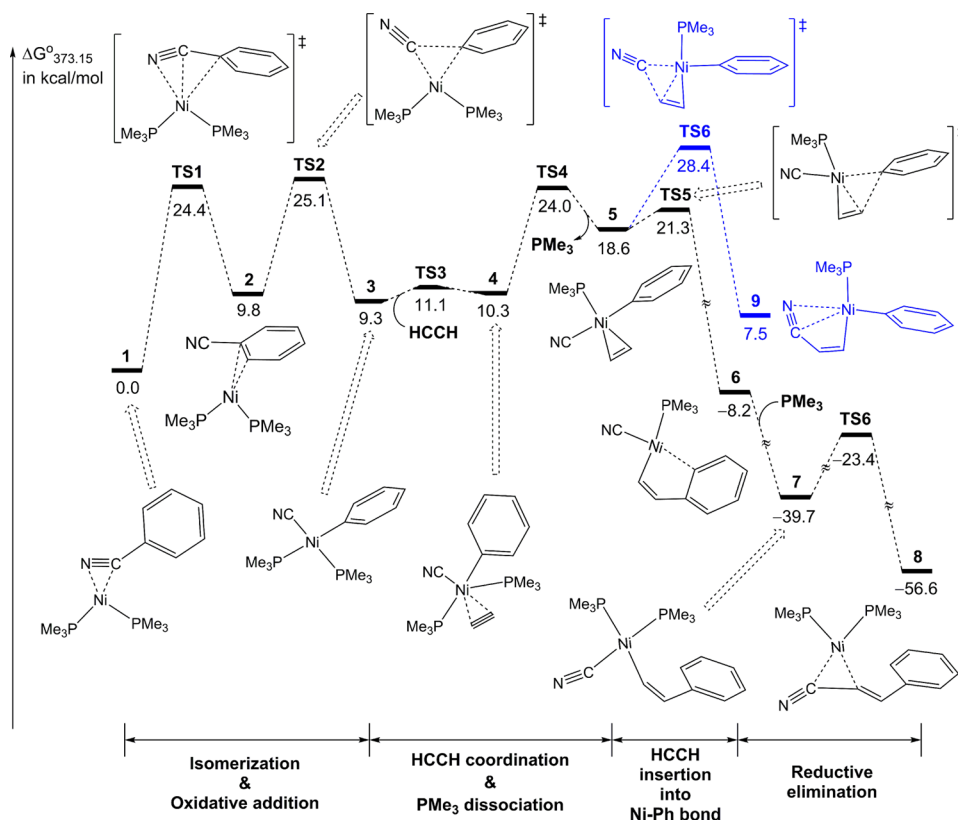
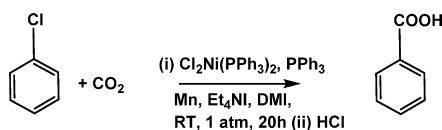


**Figure 5.** Geometry and the Gibbs energy changes (kcal/mol) in phenylcyanation of HC≡CH by Ni(PMe<sub>3</sub>)<sub>2</sub>. Bond lengths are in angstroms and bond angles in degrees.<sup>42</sup>

halide have been limited to several pioneering works such as carboxylation of aryl iodide<sup>43a</sup> and aryl bromide.<sup>43b</sup>

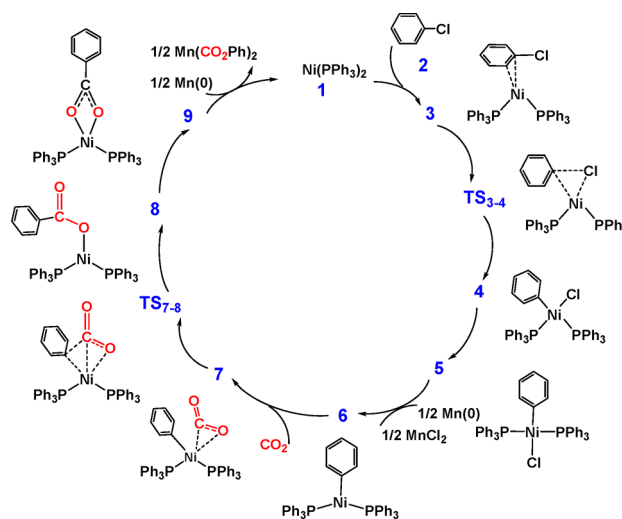
Recently, direct carboxylation of phenyl chloride<sup>44</sup> has been succeeded experimentally using a nickel(0) complex with manganese metal powder; see Scheme 21. A similar

#### Scheme 21. Nickel(0)-Catalyzed Carboxylation of Phenyl Chloride with CO<sub>2</sub>



carboxylation of benzyl chloride has also been succeeded using a nickel(0) complex with zinc powder.<sup>45</sup> However, the mechanistic details have not been clear. To elucidate the reaction mechanism, this nickel(0)-catalyzed carboxylation of phenyl chloride has been theoretically investigated recently.<sup>46</sup> The total catalytic cycle is shown in Scheme 22. The first step is the oxidative addition of phenyl chloride to Ni(PPh<sub>3</sub>)<sub>2</sub> to afford a nickel(II) intermediate, Ni(Cl)(Ph)(PPh<sub>3</sub>)<sub>2</sub>. In the nickel(0)-catalyzed phenylcyanation of alkyne, the next step is alkyne insertion, which occurs easily, as discussed above. However, CO<sub>2</sub> insertion into the Ni<sup>II</sup>–Ph bond is difficult unlike alkyne insertion. The next step is one-electron reduction of Ni(Cl)(Ph)(PPh<sub>3</sub>)<sub>2</sub> with manganese, which generates a nickel(I) intermediate, Ni<sup>I</sup>(Ph)(PPh<sub>3</sub>)<sub>2</sub> (6). Prior to CO<sub>2</sub> insertion into the Ni<sup>I</sup>–Ph bond, CO<sub>2</sub> binds with the Ni<sup>I</sup> atom in an η<sup>2</sup>-coordination mode to afford Ni<sup>I</sup>(Ph)(η<sup>2</sup>-CO<sub>2</sub>)(PPh<sub>3</sub>)<sub>2</sub> (7). From 7, CO<sub>2</sub> is easily inserted into the Ni<sup>I</sup>–Ph bond with a very small ΔG<sup>‡</sup> value to afford a nickel(I) carboxylate

#### Scheme 22. Catalytic Cycle of Nickel(0)-Catalyzed Carboxylation of Phenyl Chloride with CO<sub>2</sub>

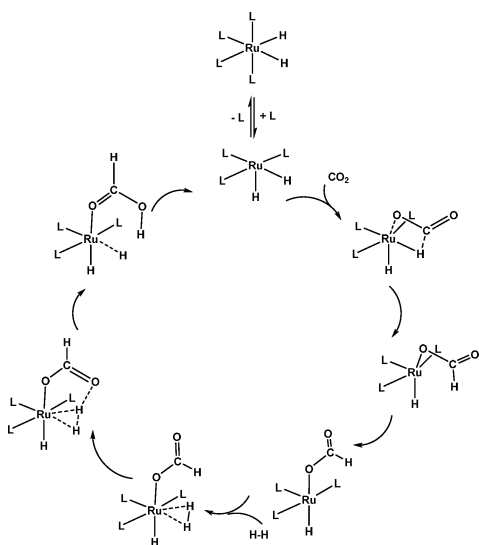


complex, Ni<sup>I</sup>(η<sup>2</sup>-O<sub>2</sub>CPh)(PPh<sub>3</sub>)<sub>2</sub> (9). One-electron reduction of 9 occurs to form a desirable product, manganese carboxylate, and regenerate an active species, Ni(PPh<sub>3</sub>)<sub>2</sub>. The rate-determining step is the concerted oxidative addition of phenyl chloride to Ni(PPh<sub>3</sub>)<sub>2</sub>. These results indicate that one-electron reduction of nickel(II) to nickel(I) is crucial for CO<sub>2</sub> insertion. This is because CT much more easily occurs from the Ni<sup>I</sup>–Ph bond to CO<sub>2</sub> than from the Ni<sup>II</sup>–Ph bond; remember that CO<sub>2</sub> insertion needs significantly large CT from the M–R moiety to CO<sub>2</sub>.<sup>47</sup> These results suggest that the efficiency of the catalytic

reaction can be improved by one-electron reduction of a nickel(II) species when the insertion reaction is difficult.

**6.2. Catalytic Reactions via Heterolytic  $\sigma$ -Bond Activation.** *A. Ruthenium(II)-Catalyzed Hydrogenation of  $\text{CO}_2$ .* Heterolytic  $\sigma$ -bond activation is also found as a crucial step in catalytic reactions. One interesting example is hydrogenation of  $\text{CO}_2$  into formic acid by a ruthenium(II) complex.<sup>48</sup> The overall reaction takes place via  $\text{CO}_2$  insertion into the  $\text{Ru}^{\text{II}}\text{-H}$  bond of  $\text{cis-Ru}(\text{H})_2(\text{PMe}_3)_3$  to form a ruthenium(II)  $\eta^1$ -formate intermediate,  $\text{Ru}(\text{H})(\eta^1\text{-OCOH})(\text{PMe}_3)_3$ ,  $\text{H}_2$  coordination to the ruthenium(II)  $\eta^1$ -formate complex, isomerization of the intermediate, and the reaction of  $\eta^1$ -formate with a  $\text{H}_2$  molecule to afford formic acid (Scheme 23).<sup>49</sup> In the formation step of formic acid, four reaction

**Scheme 23. Catalytic Cycle of Ruthenium(II)-Catalyzed Hydrogenation of  $\text{CO}_2$** <sup>48</sup>

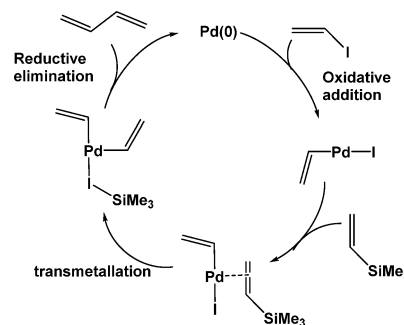


courses, such as three- and five-membered reductive eliminations and four- and six-membered  $\sigma$ -bond metatheses, are considered to be possible.<sup>49</sup> The most favorable pathway is the six-membered  $\sigma$ -bond metathesis in which the  $\text{H-H}$  bond is cleaved in a heterolytic manner. This reaction is essentially the same as the heterolytic  $\text{C-H}$   $\sigma$ -bond activation of benzene by a palladium(II) acetate complex; see above. The experimental result reported that the reaction rate depends on the  $\text{H}_2$  pressure, suggesting that  $\text{H}_2$  participates in the rate-determining step. Density functional theory (DFT) calculations indicated that the rate-determining step is  $\text{CO}_2$  insertion in the absence of a water molecule, which is seemingly inconsistent with the experimental suggestion. However, the ruthenium(II)  $\eta^1$ -formate intermediate is stabilized by  $\text{H}_2$  coordination with the Ru center. If not, deinsertion of  $\text{CO}_2$  easily occurs. These results indicate that the participation of  $\text{H}_2$  is necessary, as experimentally reported. Further theoretical study of hydrogenation of  $\text{CO}_2$  by rhodium(III), ruthenium(II), and rhodium(I) complexes indicated that  $\text{H-H}$   $\sigma$ -bond cleavage occurs through either heterolytic activation or oxidative addition, depending on the kind of metal center.<sup>50</sup>

*B. Hiyama Cross-Coupling Reaction: Crucial Role of a Fluoride Anion in  $\sigma$ -Bond Activation.* The cross-coupling reaction is of considerable importance in organic synthesis.<sup>51</sup> In general, the cross-coupling reaction occurs through the oxidative addition of a substrate to a metal atom, trans-

metalation with an organometallic compound, and reductive elimination. In transmetalation, metal oxidation state does not change at all, suggesting that  $\sigma$ -bond cleavage occurs in a heterolytic manner. Such transmetalation has been theoretically investigated in detail in the Hiyama cross-coupling reaction, which is useful for the synthesis of conjugated butadiene derivatives.<sup>52</sup> In this cross-coupling reaction, an organosilicon compound is used as one reagent.<sup>53</sup> However, the yield of product was not high because the  $\text{Si-C}$  bond is strong and it is not polarized very much. Interestingly, Hatanaka and Hiyama found that the addition of a fluoride anion to the reaction system increases the yield of product.<sup>52</sup> To clarify the reason why a fluoride anion accelerates the Hiyama cross-coupling reaction, Sakaki and co-workers theoretically investigated this reaction using vinyl iodide and trimethylvinylsilane as substrates.<sup>54</sup> The first step is the oxidative addition of vinyl iodide to a palladium(0) complex,  $\text{Pd}(\text{PMe}_3)_2$ , as shown in Scheme 24. The next step is transmetalation between

**Scheme 24. Catalytic Cycle of the Hiyama Cross-Coupling Reaction**



$\text{PdI}(\text{CH}=\text{CH}_2)(\text{PMe}_3)_2$  and trimethylvinylsilane,  $\text{CH}_2=\text{CH-SiMe}_3$ . This transmetalation is the same as heterolytic  $\sigma$ -bond activation of the  $\text{Si-vinyl}$  bond. In the absence of a fluoride anion, transmetalation needs a very large barrier, which is a rate-determining step. In the presence of tetramethylammonium fluoride, two reaction courses are possible; in one, substitution of a fluoride anion for an iodide anion occurs in  $\text{PdI}(\text{CH}=\text{CH}_2)(\text{PMe}_3)_2$  to afford  $\text{PdF}(\text{CH}=\text{CH}_2)(\text{PMe}_3)_2$ . In another, the fluoride anion approaches the Si atom of  $\text{CH}_2=\text{CH-SiMe}_3$  to activate the  $\text{Si-CH}=\text{CH}_2$  bond. In both cases, transmetalation occurs with a moderate activation barrier, indicating that a fluoride anion accelerates transmetalation. The moderate activation barrier was discussed in terms of the formation of a strong  $\text{Si-F}$  bond and also stabilization of the TS by formation of hypervalent silicon species because the hypervalent species needs in general the presence of an electronegative group on the Si center. A similar stabilization of the TS was observed in catalytic hydrosilylation of ketone and  $\text{CO}_2$  by a germanium hydride compound, in which the hypervalent silicon species is formed in the TS of heterolytic  $\text{Si-H}$   $\sigma$ -bond activation.<sup>55</sup> These results suggest that not only a fluoride anion but also an electronegative group accelerate the Hiyama cross-coupling reaction and similar reactions.

Heterolytic  $\sigma$ -bond activation also participates in a palladium(II)-catalyzed direct cross-coupling reaction.<sup>56</sup> Theoretical calculations were recently performed to elucidate the reaction mechanism and electronic process.<sup>57,58</sup> However, we skip the discussion of these reactions because  $\text{C-H}$  activation involved in these reactions is discussed in the other part of this Forum.

## 7. PERSPECTIVE

Because the  $\sigma$ -bond activation reaction is one of the important reactions in inorganic chemistry, organometallic chemistry, and catalytic chemistry, many theoretical studies have been performed. In particular, the concerted oxidative addition has been well investigated. However, many issues to be investigated still remain. For instance, the regioselectivity of the concerted oxidative addition has not been theoretically investigated well. Also, the oxidative addition to M–L must be investigated experimentally and theoretically because recent reports by the Peters group indicates the importance of this reaction.<sup>35</sup>

From the viewpoint of the computational method, solvation effects must be correctly considered in heterolytic  $\sigma$ -bond activation and oxidative addition via the nucleophilic attack of M. In both reactions, solvation effects play crucial roles in stabilizing the TS and intermediate. In many works, PCM and similar methods are used now because they are effective and useful for evaluating the solvation effects with reasonable computational cost. However, the 3D-RISM-SCF and QM/MM-MD simulations, which have been used in the theoretical study of biological systems,<sup>59</sup> are also very effective for transition-metal systems.<sup>60</sup> The use of those methods would provide us more detailed knowledge of solvation.

In this short review, we could not have enough space to describe all  $\sigma$ -bond activation reactions. For instance, we skipped theoretical studies of heterolytic C–H  $\sigma$ -bond activation by metal oxides<sup>61</sup> and heterolytic  $\sigma$ -bond activation of H<sub>2</sub> in biological systems.<sup>62</sup> Recently, the electrochemical formation of a H<sub>2</sub> molecule has attracted a lot of interest. This reaction is considered to be the reverse of heterolytic  $\sigma$ -bond activation of the H–H bond of a H<sub>2</sub> molecule in many cases. Another important theoretical viewpoint is that  $\sigma$ -bond activation occurs via singlet coupling of two radical centers. Such an investigation is presented by a theoretical study of the conversion of cyclopropene to vinylcarbene by a ruthenium(II) complex.<sup>63</sup> In this work, several singlet couplings of unpaired electrons were discussed based on the CASVB method.

We believe that theoretical knowledge of the  $\sigma$ -bond activation reaction is indispensable for the further development of inorganic, organometallic, and catalytic chemistry.

## AUTHOR INFORMATION

### Corresponding Author

\*E-mail: sakaki.shigeyoshi.47e@st.kyoto-u.ac.jp.

### Author Contributions

All others are common authors; they are presented in alphabetical order.

### Notes

The authors declare no competing financial interest.

## ACKNOWLEDGMENTS

This work is financially supported, in part, by Grant-in-Aids of Specially Promoted Science and Technology (Grant 22000009) and the Grand Challenge Project (IMS) from Ministry of Education, Culture, Science, Sports, and Technology.

## REFERENCES

(1) For instance, see: (a) Lyons, T. W.; Sanford, M. S. *Chem. Rev.* **2010**, *110*, 1147–1169. (b) Ackermann, L. *Chem. Rev.* **2011**, *111*, 1315–1345. (c) Partyka, D. V. *Chem. Rev.* **2011**, *111*, 1529–1595. (d) Arockiam, P. B.; Bruneau, C.; Dixneuf, P. H. *Chem. Rev.* **2012**, *112*, 5879–5918.

(2) (a) Sakaki, S.; Ochi, N.; Ohnishi, Y. Heterolytic  $\sigma$ -Bond Activation by Transition Metal Complexes. In *Computational Modeling for Homogeneous and Enzymatic Catalysis*; Morokuma, K., Musaev, D. J., Eds.; Wiley-VCH: Weinheim, Germany, 2008; pp 265–284. (b) Sakaki, S.; Sato, H.; Ohnishi, Y.-y. *Chem. Rec.* **2010**, *10*, 29–45. (b) Sakaki, S. Theoretical Study of  $\sigma$ -Bond Activation Reactions and Catalytic Reactions by Transition Metal Complexes. In *Practical Aspects of Computational Chemistry II*; Leszczynski, J., Shukla, M. K., Eds.; Springer: Berlin, 2012; pp391–470.

(3) Cui, Q.; Musaev, D. G.; Morokuma, K. *Organometallics* **1998**, *17*, 1383–1392.

(4) (a) Sakaki, S.; Takayama, T.; Sugimoto, M. *Chem. Lett.* **2001**, *30*, 1222–1223. (b) Sakaki, S.; Takayama, T.; Sumimoto, T.; Sugimoto, M. *J. Am. Chem. Soc.* **2004**, *126*, 3332–3348.

(5) Tatsumi, K.; Hoffmann, R.; Yamamoto, A.; Still, J. K. *Bull. Chem. Soc. Jpn.* **1981**, *54*, 1857–1867.

(6) Ochi, N.; Nakao, Y.; Sato, S.; Sakaki, S. *J. Am. Chem. Soc.* **2007**, *129*, 8615–8624.

(7) Obara, S.; Kitaura, K.; Morokuma, K. *J. Am. Chem. Soc.* **1984**, *106*, 7482–7492.

(8) Ohnishi, Y. Y.; Nakao, Y.; Sato, H.; Sakaki, S. *J. Phys. Chem. A* **2007**, *111*, 7915–7924.

(9) Devarajan, D.; Ess, D. H. *Inorg. Chem.* **2012**, *51*, 6367–6375.

(10) Sakaki, S.; Mizoe, N.; Musashi, Y.; Biswas, B.; Sugimoto, M. *J. Phys. Chem. A* **1998**, *102*, 8027–8036.

(11) Sakaki, S.; Kai, S.; Sugimoto, M. *Organometallics* **1999**, *18*, 4825–4837.

(12) Ariafard, A.; Lin, Z. *Organometallics* **2006**, *25*, 4030–4033.

(13) (a) Sayyed, F. B.; Sakaki, S., to be published. All calculations were carried out with the B3LYP-D functional using LanL2Tz(f) for Ni, 6-31G(d) basis sets for C, H, and P, and 6-31+G(d) for Cl. We provided the stabilization energy of the precursor and the activation energy after correction of the basis set superposition error. *Gaussian09* was employed. (b) The  $\Delta G^{\circ\ddagger}$  value for the oxidative addition of Ph–Cl to Pd(PPh<sub>3</sub>)<sub>2</sub> is somewhat smaller than the value of ref 17a but similar to that of ref 17b. Considering that this oxidative addition does not occur experimentally, the  $\Delta G^{\circ\ddagger}$  value is large. We need to carefully check the reliability of DFT functionals for this type of reaction. However, a comparison of the reactivity between M(PR<sub>3</sub>)<sub>2</sub> and M(PR<sub>3</sub>) can be discussed well based on all of the computational values reported in refs <sup>17a</sup> and <sup>17b</sup> and our work.

(14) Ateşin, T. A.; Li, T.; Lachaize, S.; Brennessel, W. W.; García, J. J.; Jones, W. D. *J. Am. Chem. Soc.* **2007**, *129*, 7562–7569.

(15) Ohnishi, Y.-Y.; Nakao, Y.; Sato, H.; Sakaki, S. *J. Phys. Chem. A* **2007**, *111*, 7915–7924.

(16) (a) Christmann, U.; Vilar, R. *Angew. Chem., Int. Ed.* **2005**, *44*, 366–374. (b) Hartwig, J. F. *Angew. Chem., Int. Ed.* **1998**, *37*, 2046–2067. (c) Galardon, E.; Ramdeehul, S.; Brown, J. M.; Cowley, A.; Hii, K. K.; Jutand, A. *Angew. Chem., Int. Ed.* **2002**, *41*, 1760–1763. (d) Stambuli, J. P.; Buehl, M.; Hartwig, J. F. *J. Am. Chem. Soc.* **2002**, *124*, 9346–9347. (e) Stambuli, J. P.; Incarvito, C. D.; Buehl, M.; Hartwig, J. F. *J. Am. Chem. Soc.* **2004**, *126*, 1184–1194. (f) Yamashita, M.; Hartwig, J. F. *J. Am. Chem. Soc.* **2004**, *126*, 5344–5345.

(17) (a) Li, Z.; Fu, Y.; Guo, Q.-X.; Liu, L. *Organometallics* **2008**, *27*, 4043–4049. (b) Vikse, K.; Naka, T.; McIndoe, J. S.; Besora, M.; Maseras, F. *ChemCatChem* **2013**, *5*, 3604–3609.

(18) Correa, A.; Cornella, J.; Martin, R. *Angew. Chem., Int. Ed.* **2013**, *52*, 1878–1880 and references cited therein.

(19) For instance, see: (a) Yoshino, Y.; Kurahashi, T.; Matubara, S. *J. Am. Chem. Soc.* **2009**, *131*, 7494–7495. (b) Nakai, K.; Kurahashi, T.; Matubara, S. *J. Am. Chem. Soc.* **2011**, *133*, 11066–11068.

(20) Guan, W.; Sakaki, S.; Kurahashi, T.; Matubara, S. *Organometallics* **2013**, *32*, 7564–7574.

(21) (a) The stepwise oxidative addition was first reported by Rzepa and co-workers.<sup>21b</sup> They found the presence of the zwitterionic intermediate before  $\sigma$ -bond cleavage. However, it is not clear whether  $\sigma$ -bond cleavage occurs in one step or in a stepwise manner via nucleophilic attack. They recognized that the presence of electron-withdrawing substitution and the solvation effect are important for the

- zwitterionic intermediate. (b) Jakt, M.; Johannissen, L.; Rzepa, H. S.; Widdowson, D. A.; Wilhelm, R. *J. Chem. Soc., Perkin Trans. 2* **2002**, 576–581.
- (22) Senn, H. M.; Ziegler, T. *Organometallics* **2004**, *23*, 2980–2988.
- (23) (a) Kégl, T.; Kollar, L. *J. Organomet. Chem.* **2007**, *692*, 1852–1858. (b) Rendina, L. M.; Puddephatt, R. *J. Chem. Rev.* **1997**, *97*, 1735–1754.
- (24) Hayaki, S.; Yokogawa, D.; Sato, H.; Sakaki, S. *Chem. Phys. Lett.* **2008**, *458*, 329–332.
- (25) Zeng, G.; Sakaki, S. *Inorg. Chem.* **2011**, *50*, 5290–5297.
- (26) Braunschweig, H.; Radacki, K.; Schneider, A. *Science* **2010**, *328*, 345–347.
- (27) Tsukamoto, S.; Sakaki, S. *J. Phys. Chem. A* **2011**, *115*, 8520–8527.
- (28) (a) Sakaki, S.; Dedieu, A. *Inorg. Chem.* **1987**, *26*, 3278–3284. (b) Sakaki, S.; Aizawa, T.; Koga, K.; Morokuma, K.; Ohkubo, K. *Inorg. Chem.* **1989**, *28*, 103–109.
- (29) (a) Aresta, M.; Nobile, C. F.; Albano, V. G.; Forni, E.; Manassero, M. *J. Chem. Soc., Chem. Commun.* **1975**, 636–637. (b) Gambarotta, S.; Arena, F.; Floriani, C.; Zanazzi, P. F. *J. Am. Chem. Soc.* **1982**, *104*, 5082–5092. (c) Herskovitz, T.; Guggenberger, L. *J. Am. Chem. Soc.* **1976**, *98*, 1615–1616. (d) Calabrese, J. C.; Herskovitz, T.; Kinney, J. B. *J. Am. Chem. Soc.* **1983**, *105*, 5914–5915.
- (30) (a) Moritani, I.; Fujiwara, Y. *Tetrahedron Lett.* **1967**, *8*, 1119–1122. (b) Fujiwara, Y.; Moritani, I.; Matsuda, M. *Tetrahedron Lett.* **1968**, *9*, 633–636. (c) Fujiwara, Y.; Takaki, K.; Taniguchi, Y. *Synlett* **1996**, 591–599 and references cited therein.
- (31) Biswas, B.; Sugimoto, M.; Sakaki, S. *Organometallics* **2000**, *19*, 3895–3908.
- (32) Garcia-Cuadrado, D.; Braga, A. A. C.; Maseras, F.; Echavarren, A. M. *J. Am. Chem. Soc.* **2006**, *128*, 1066–1067.
- (33) Davies, D. L.; Donald, S. M. A.; Macgregor, S. A. *J. Am. Chem. Soc.* **2005**, *127*, 13754–13755.
- (34) Campeau, L. C.; Rousseaux, S.; Fagnou, K. *J. Am. Chem. Soc.* **2005**, *127*, 18020–18021.
- (35) (a) Harman, W. H.; Peters, J. C. *J. Am. Chem. Soc.* **2012**, *134*, 5080–5082. (b) Harman, W. H.; Lin, T. P.; Peters, J. C. *Angew. Chem., Int. Ed.* **2014**, *53*, 1081–1086.
- (36) (a) Green, M. L. H. *J. Organomet. Chem.* **1995**, *500*, 127–148. (b) Parkin, G. *Organometallics* **2006**, *25*, 4744–4747. (c) Amgoune, A.; Bourissou, D. *Chem. Commun.* **2011**, *47*, 859–871.
- (37) Zeng, G.; Sakaki, S. *Inorg. Chem.* **2013**, *52*, 2844–2853.
- (38) (a) Pang, K.; Tanski, J. M.; Parkin, G. *Chem. Commun.* **2008**, 1008–1010. (b) Figueroa, J. S.; Melnick, J. G.; Parkin, G. *Inorg. Chem.* **2006**, *45*, 7056–7058. (c) Pang, K.; Quan, S. M.; Parkin, G. *Chem. Commun.* **2006**, 5015–5017.
- (39) Tsoureas, N.; Kuo, Y.; Haddow, M. F.; Owen, G. R. *Chem. Commun.* **2011**, *47*, 484–486.
- (40) (a) Nakao, Y.; Oda, S.; Hiyama, T. *J. Am. Chem. Soc.* **2004**, *126*, 13904–13905. (b) Nakao, Y.; Oda, S.; Yada, A.; Hiyama, T. *Tetrahedron* **2006**, *62*, 7567–7576.
- (41) Ateşin, T. A.; Li, T.; Lachaize, S.; García, J. J.; Jones, W. D. *Organometallics* **2008**, *27*, 3811–3817.
- (42) Ohnishi, Y.-Y.; Nakao, Y.; Sato, H.; Nakao, Y.; Hiyama, T.; Sakaki, S. *Organometallics* **2009**, *28*, 2583–2594.
- (43) (a) Tran-Vu, H.; Daugulis, O. *ACS Catal.* **2013**, *3*, 2417–2420. (b) Correa, A.; Martín, R. *J. Am. Chem. Soc.* **2009**, *131*, 15974–15975.
- (44) Fujihara, T.; Nogi, K.; Xu, T.; Terao, J.; Tsuji, Y. *J. Am. Chem. Soc.* **2012**, *134*, 9106–9109.
- (45) León, T.; Correa, A.; Martín, R. *J. Am. Chem. Soc.* **2013**, *135*, 1221–1224.
- (46) Sayyed, F. B.; Tsuji, Y.; Sakaki, S. *Chem. Commun.* **2013**, *49*, 10715–10717.
- (47) (a) Sakaki, S.; Ohkubo, K. *Inorg. Chem.* **1988**, *27*, 2020–2021. (b) Sakaki, S.; Ohkubo, K. *Organometallics* **1989**, *8*, 2970–2973. (c) Sakaki, S.; Ohkubo, K. *Inorg. Chem.* **1989**, *28*, 2583–2590.
- (48) Jessop, P. G.; Ikariya, T.; Noyori, R. *Nature* **1994**, *368*, 231–233.
- (49) (a) Musashi, Y.; Sakaki, S. *J. Am. Chem. Soc.* **2000**, *122*, 3867–3877. (b) Ohnishi, Y. Y.; Matsunaga, T.; Nakao, Y.; Sato, H.; Sakaki, S. *J. Am. Chem. Soc.* **2005**, *127*, 4021–4032. (c) Ohnishi, Y. Y.; Nakao, Y.; Sato, H.; Sakaki, S. *Organometallics* **2006**, *25*, 3352–3363.
- (50) Musashi, Y.; Sakaki, S. *J. Am. Chem. Soc.* **2002**, *124*, 7588–7603.
- (51) For instance, see: (a) Miyaoura, N.; Suzuki, A. *Chem. Rev.* **1995**, *95*, 2457–2483. (b) Nakao, Y.; Hiyama, T. *Chem. Soc. Rev.* **2011**, *40*, 4893–4901.
- (52) Hatanaka, Y.; Hiyama, T. *Pure Appl. Chem.* **1994**, *66*, 1471–1478.
- (53) Hallberg, A.; Westerlund, C. *Chem. Lett.* **1982**, 1993–1994.
- (54) Sugiyama, A.; Ohnishi, Y. Y.; Nakaoka, M.; Nakao, Y.; Sato, H.; Sakaki, S.; Nakao, Y.; Hiyama, T. *J. Am. Chem. Soc.* **2008**, *130*, 12975–12985.
- (55) Takagi, N.; Sakaki, S. *J. Am. Chem. Soc.* **2013**, *135*, 8955–8965.
- (56) For instance, see: (a) Hull, K. L.; Sanford, M. S. *J. Am. Chem. Soc.* **2009**, *131*, 9651–9652. (b) Lapointe, D.; Fagnou, K. *Chem. Lett.* **2010**, *39*, 1118–1126. (c) Wakioka, M.; Nakamura, Y.; Wang, Q.; Ozawa, F. *Organometallics* **2012**, *31*, 4810–4816. (d) Tan, Y.; Barrios-Landeros, F.; Hartwig, J. F. *J. Am. Chem. Soc.* **2012**, *134*, 3683–3686.
- (57) Ishikawa, A.; Nakao, Y.; Sato, H.; Sakaki, S. *Dalton Trans.* **2010**, *39*, 3279–3289.
- (58) Wakioka, M.; Nakamura, Y.; Hihara, Y.; Ozawa, F.; Sakaki, S. *Organometallics* **2013**, *32*, 4423–4430.
- (59) (a) Yamamoto, T. *J. Chem. Phys.* **2008**, *129*, 244104. (b) Nakano, H.; Yamamoto, T. *J. Chem. Phys.* **2012**, *136*, 134107. (c) Kosugi, K.; Hayashi, S. *J. Chem. Theory Comput.* **2012**, *8*, 322–334. (d) Kosugi, K.; Hayashi, S. *J. Am. Chem. Soc.* **2012**, *134*, 7045–7055.
- (60) For instance, see: (a) Aono, S.; Sakaki, S. *J. Phys. Chem. B* **2012**, *116*, 13045–13062. (b) Aono, S.; Nakagaki, M.; Sakaki, S. *J. Chem. Theory Comput.* **2014**, *10*, 1062–1073.
- (61) (a) Yoshizawa, K.; Shiota, Y.; Yamabe, T. *J. Am. Chem. Soc.* **1998**, *120*, 564–572. (b) Yoshizawa, K.; Shiota, Y.; Yamabe, T. *Organometallics* **1998**, *17*, 2825–2831. (c) Yoshizawa, K.; Shiota, Y.; Yamabe, T. *J. Am. Chem. Soc.* **1999**, *121*, 147–153. (d) Shiota, Y.; Suzuki, K.; Yoshizawa, K. *Organometallics* **2005**, *24*, 3532–3538. (e) Böhme, D. K.; Schwarz, H. *Angew. Chem., Int. Ed.* **2005**, *44*, 2336–2354. (f) Dietl, N.; Schlangen, M.; Schwartz, H. *Chem.—Eur. J.* **2011**, *17*, 1783–1788. (g) Božović, A.; Feil, S.; Koyanagi, G. K.; Viggiano, A. A.; Zhang, X.; Schlangen, M.; Schwarz, H.; Bohme, D. K. *Chem.—Eur. J.* **2010**, *16*, 11605–11610.
- (62) (a) Siegbahn, P. E. M.; Blomberg, M. R. A.; Pavlov, M. W. N.; Crabtree, R. H. *J. Biol. Inorg. Chem.* **2001**, *6*, 460–466. (b) Siegbahn, P. E. M. *Chem. Rev.* **2007**, *107*, 4414–4435.
- (63) Ishikawa, A.; Tanimura, Y.; Nakao, Y.; Sato, H.; Sakaki, S. *Organometallics* **2012**, *31*, 8189–8199.